
Compact Memory for Continual Logistic Regression

Yohan Jung¹ Hyungi Lee^{2*} Wenlong Chen^{3*} Thomas Möllenhoff¹
Yingzhen Li³ Juho Lee⁴ Mohammad Emtiyaz Khan¹

¹RIKEN Center for AI Project ²Kookmin University

³Imperial College London ⁴KAIST

*Work performed in part during internship at the RIKEN Center for AI Project.

Abstract

Despite recent progress, continual learning still does not match the performance of batch training. To avoid catastrophic forgetting, we need to build compact memory of essential past knowledge, but no clear solution has yet emerged, even for shallow neural networks with just one or two layers. In this paper, we present a new method to build compact memory for logistic regression. Our method is based on a result by [Khan and Swaroop \[2021\]](#) who show the existence of optimal memory for such models. We formulate the search for the optimal memory as Hessian-matching and propose a probabilistic PCA method to estimate them. Our approach can drastically improve accuracy compared to Experience Replay. For instance, on Split-ImageNet, we get 60% accuracy compared to 30% obtained by replay with memory-size equivalent to 0.3% of the data size. Increasing the memory size to 2% further boosts the accuracy to 74%, closing the gap to the batch accuracy of 77.6% on this task. Our work opens a new direction for building compact memory that can also be useful in the future for continual deep learning.

1 Introduction

Continual learning aims for a continual lifelong acquisition of knowledge which is challenging because it requires a delicate balance between the old and new knowledge [[Mermillod et al., 2013](#)]. New knowledge can interfere with old knowledge [[Sutton, 1986](#)] and lead to catastrophic forgetting [[Kirkpatrick et al., 2017](#)]. Thus, it is necessary to compactly memorize all the past knowledge required in the future to quickly learn new things. This is a difficult problem and no satisfactory solution has been found yet, even for simple cases such as logistic regression and shallow neural networks. The problem is important because solving it can also drastically reduce the cost and environmental impact of batch training which requires access to all of the data all the time.

The most straightforward method to build memory is to simply store old models and data examples, but such approaches do not perform as well as batch training. For instance, weight-regularization uses old parameters to regularize future training [[Kirkpatrick et al., 2017](#), [Li and Hoiem, 2017](#), [Lee et al., 2017](#), [Zenke et al., 2017](#), [Ebrahimi et al., 2020](#), [Ritter et al., 2018](#), [Nguyen et al., 2018](#)]. While this is memory efficient, it often performs worse than replay method that simply store old raw data for reuse in the future [[Rolnick et al., 2019](#), [Lopez-Paz and Ranzato, 2017](#), [Chaudhry et al., 2019](#), [Titsias et al., 2020](#), [Buzzega et al., 2020](#), [Pan et al., 2020](#), [Scannell et al., 2024](#)]. Many replay-based methods have been devised to effectively select past data points based on gradient [[Aljundi et al., 2019a](#), [Yoon et al., 2022](#)], interference [[Aljundi et al., 2019b](#)], information-theoretic metric [[Sun et al., 2022](#)], and Bilevel optimization [[Borsos et al., 2020](#)]. The memory cost of replay can be reduced by combining it with weight regularization, but so far the performance still lags behind the batch training [[Daxberger et al., 2023](#)]. The goal of this work is to propose new methods to build compact memory for the

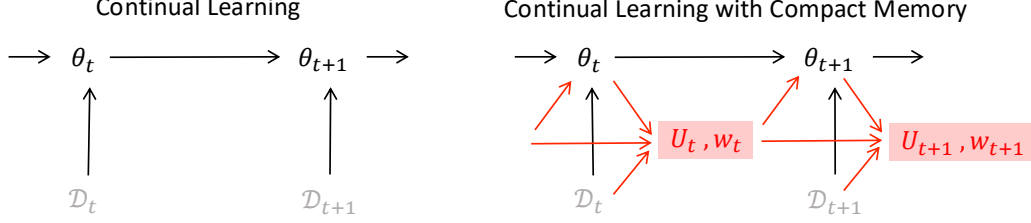


Figure 1: Standard continual-learning methods, such as those using weight regularization, use past parameters θ_t to update θ_{t+1} for the new task \mathcal{D}_{t+1} (shown on the left). We propose a new method (shown on the right) that also builds compact memory and reuses it to continually learn. The memory consists of a set \mathbf{U}_t of memory vectors and a weight vector \mathbf{w}_t . These are used to update θ_{t+1} when new \mathcal{D}_{t+1} arrives. Afterward, the memory is updated to get the new $(\mathbf{U}_{t+1}, \mathbf{w}_{t+1})$.

simplest non-trivial case of logistic regression. With this, we hope to gain new insights to be able to do the same in the future for continual deep learning.

We build upon the work of Khan and Swaroop [2021] who show the existence of compact memory for logistic regression but do not give a practical method to estimate them. They propose a prior called the Knowledge-adaptation prior (K-prior) which uses a ‘memory’ set to approximate the full-batch gradient. More precisely, given parameter θ_t after training until task t , a subset \mathcal{M}_t of the past data $\mathcal{D}_{1:t} = \{\mathcal{D}_1, \mathcal{D}_2, \dots, \mathcal{D}_t\}$ is used to construct the K-prior $\mathcal{K}_t(\theta; \mathcal{M}_t)$ such that the following holds:

$$\sum_{j=1}^t \nabla \bar{\ell}_j(\theta; \mathcal{D}_j) \approx \nabla \mathcal{K}_t(\theta; \mathcal{M}_t), \quad (1)$$

where $\bar{\ell}_j(\theta; \mathcal{D}_j)$ denotes the loss over examples in \mathcal{D}_j . Khan and Swaroop [2021, App. A] show that, for logistic regression, it is also possible to construct an *optimal* memory by using the singular vectors of the feature matrix. The optimality refers to the fact that the memory can, in theory, *perfectly* recover full-batch gradient, that is, the approximation in Eq. 1 becomes an equality. The optimal memory size depends on the rank of the feature matrix, not on the size of whole $\mathcal{D}_{1:t}$, yielding a compact optimal memory. The main issue with the method is that it requires access to the whole $\mathcal{D}_{1:t}$ to construct the memory which is not possible when learning continually. Our goal here is to propose a practical alternative to estimate such memory for continual logistic regression.

In this paper, we reformulate the search for the optimal memory as Hessian-matching and propose a practical method to estimate them (Fig. 1). We are motivated by the fact that, in linear regression, estimation of optimal memory can be reformulated as Hessian matching. We generalize this to logistic regression by posing it as a maximum likelihood estimation problem which uses the classical Probabilistic Principal Component Analysis [PPCA; Tipping and Bishop, 1999a]. The method does not yield perfect gradient reconstruction anymore, but can still drastically improve performance compared to replay of raw old data. For instance, on the Split-ImageNet dataset, we obtain 60% accuracy compared to the 30% accuracy obtained by replay with memory-size equivalent to 0.3% of the data size. A small memory size of 2% of the data size is sufficient to obtain an accuracy of 74%, closing the gap to the batch accuracy of 77.6% on this task. Our work opens a new direction for building compact memory that can also be useful in the future for continual deep learning. Our code is available at https://github.com/team-approx-bayes/compact_memory_code.

2 Compact Memory for Continual Learning

We consider continual learning for supervised problems where the data of the j ’th task consists of N_j input-output pairs of form (\mathbf{x}_j, y_j) . The goal is to learn the parameter vector θ whose predictions closely match the true labels y_j . The empirical loss over task j is defined as

$$\bar{\ell}_j(\theta; \mathcal{D}_j) = \sum_{i \in \mathcal{D}_j} \mathcal{L}(y_j, \hat{y}(f_{\theta}(\mathbf{x}_j))), \quad (2)$$

where $\mathcal{L}(y, \hat{y})$ is chosen to be the cross-entropy loss over predictions \hat{y} obtained by passing the logits $f_{\theta}(\mathbf{x})$ through the softmax function. As discussed earlier, learning continually requires a delicate

balance between old and new knowledge. Tasks may arrive one at a time and there may be little flexibility to revisit them again. This is unlike the standard ‘batch’ training where the goal is to obtain the parameter θ_T^* obtained by jointly training over the sum $\sum_{j=1}^T \ell_j$ over all T tasks. Such batch training typically requires access to all the data all the time. Continual learning eliminates this requirements and aim to recover θ_T^* by incrementally training of tasks one at a time.

Continual learning however is extremely challenging, even for simple cases such as logistic regression and shallow neural networks. If new task interferes with the old knowledge, there is a chance the model may catastrophically forget the previously acquired knowledge. Because the tasks are not revisited, the model may never be able to relearn it. It is therefore important to compactly memorize all essential knowledge that may be needed to learn new things in the future. This is challenging because the future is uncertain and new tasks may be very different from old ones. No satisfactory solution has been found yet to build compact memory that facilitates accurate continual learning.

Currently, there are two most popular methods to build memory and both do not perform as well as batch training. The first method is to store the old model parameters θ_t after training until task t and reuse it to train over the next task. For example, we can use a quadratic weight-regularizer:

$$\theta_{t+1} \leftarrow \arg \min_{\theta} \bar{\ell}_{t+1}(\theta; \mathcal{D}_{t+1}) + \frac{1}{2} \delta_t \|\theta - \theta_t\|^2, \quad (3)$$

where $\delta_t > 0$ is the regularization parameter. This is memory efficient because the memory cost does not grow with tasks and requires storing only one model parameters. It is also possible to use multiple checkpoints as long as the memory does not grow too fast.

The second method is to store old raw data, which is often not the most memory efficient approach. This is because the memory size could grow larger as new tasks are seen. However, in practice, the method often performs much better than weight regularization. The method is also easy to implement within standard stochastic training pipeline. For instance, given a set \mathcal{E}_t of replay examples, we can simply us the following update,

$$\theta_{t+1} \leftarrow \arg \min_{\theta} \bar{\ell}_{t+1}(\theta; \mathcal{D}_{t+1}) + \sum_{j \in \mathcal{E}_t} \mathcal{L}(y_j, \hat{y}(f_{\theta}(\mathbf{x}_j))). \quad (4)$$

Another alternative is to use a *function-space* regularizer, defined as $\mathcal{L}(\hat{y}(f_{\theta_t}(\mathbf{x}_j)), \hat{y}(f_{\theta}(\mathbf{x}_j)))$ where instead of predicting the true labels y_j , we predict prediction $\hat{y}(f_{\theta_t}(\mathbf{x}_j))$ of θ_t . This also boosts performance in practice [Titsias et al., 2020, Buzzega et al., 2020, Pan et al., 2020, Scannell et al., 2024]. The memory efficiency of all of these methods can be reduced by combining them with weight regularization, which brings us to the Knowledge-adaptation prior of Khan and Swaroop [2021].

As discussed earlier, K-prior uses both θ_t and a memory set \mathcal{M}_t to approximate the full-batch gradient over the past tasks. The memory set consists of K_t vectors, that is, $\mathcal{M}_t = (\mathbf{u}_{1|t}, \mathbf{u}_{2|t}, \dots, \mathbf{u}_{K_t|t})$ where $\mathbf{u}_{k|t}$ is the k ’th memory vector. K-prior uses a combination of the weight-space and function-space regularizer to approximate the full-batch gradient. For instance, consider a regularized linear-regression problem with loss $\mathcal{L}(y_j, \hat{y}(\phi_j^\top \theta)) = \frac{1}{2} (y_j - \phi_j^\top \theta)^2$ for each (ϕ_j, y_j) pair, with a regularizer $\frac{1}{2} \delta_t \|\theta\|^2$. For this model, we can use the following combination:

$$\mathcal{K}_t(\theta; \mathcal{M}_t) = \frac{1}{2} \delta_t \|\theta - \theta_t\|^2 + \sum_{k=1}^{K_t} \frac{1}{2} \left(\mathbf{u}_{k|t}^\top \theta_t - \mathbf{u}_{k|t}^\top \theta \right)^2. \quad (5)$$

The first term ensures that new θ are close to old θ_t while the second term ensures the same for their predictions. We then use the following update for the next task,

$$\theta_{t+1} \leftarrow \arg \min_{\theta} \bar{\ell}_{t+1}(\theta; \mathcal{D}_{t+1}) + \mathcal{K}_t(\theta; \mathcal{M}_t). \quad (6)$$

Khan and Swaroop [2021] prove that, for generalized linear models, such an update can perfectly recover the exact gradient when $\mathcal{M}_t = \mathcal{D}_{1:t}$ and $\theta_t = \theta_t^*$ (the batch solution over $\mathcal{D}_{1:t}$). Choosing a subset of $\mathcal{D}_{1:t}$ as the memory set yields an approximation of the gradient whose accuracy can be controlled by carefully choosing the memory set, as long as θ_t is close enough to θ_t^* .

Choosing $\mathcal{M}_t \subset \mathcal{D}_{1:t}$ however is not the best choice. Khan and Swaroop [2021, App. A] show that it is also possible to construct a much more compact *optimal* memory set which can recover prefect gradients even when $|\mathcal{M}_t| \ll |\mathcal{D}_{1:t}|$. This can be done by setting $\mathbf{u}_{k|t}$ to be the left singular vectors of the feature matrix. To be precise, denoting by $\Phi_{1:t}$ the feature matrix of containing features of inputs in $\mathcal{D}_{1:t}$ as columns, we compute the following singular-value-decomposition (SVD),

$$\Phi_{1:t} = \mathbf{U}_t^* \mathbf{S}_t^* (\mathbf{V}_t^*)^\top, \text{ where } \mathbf{U}_t^* = (\mathbf{u}_{1|t}^*, \mathbf{u}_{2|t}^*, \dots, \mathbf{u}_{K_t^*|t}^*) \text{ and } \mathbf{V}_t^* = (\mathbf{v}_{1|t}^*, \mathbf{v}_{2|t}^*, \dots, \mathbf{v}_{K_t^*|t}^*). \quad (7)$$

The left and right singular vectors are denoted by \mathbf{u}_t^* and $\mathbf{v}_{k|t}^*$ respectively. The rank is denoted by K_t^* and \mathbf{S}_t^* is a diagonal matrix containing all K_t^* non-zero singular values denoted by $s_{k|t}^*$. Khan and Swaroop [2021, App. A] define the optimal memory to be $\mathcal{M}_t = \mathbf{U}_t^*$. Then, they construct the following optimal K-prior, denoted by $\mathcal{K}_t^*(\boldsymbol{\theta}; \mathbf{U}_t^*)$, for binary logistic regression,

$$\mathcal{K}_t^*(\boldsymbol{\theta}; \mathbf{U}_t^*) = \frac{1}{2}\delta\|\boldsymbol{\theta} - \boldsymbol{\theta}_t\|^2 + \sum_{k=1}^{K_t^*} w_{k|t}^* \mathcal{L}\left(\hat{y}((\mathbf{u}_{k|t}^*)^\top \boldsymbol{\theta}_t), \hat{y}((\mathbf{u}_{k|t}^*)^\top \boldsymbol{\theta})\right), \quad (8)$$

and show that there exist scalars $w_{k|t}^*$ for which it perfectly recovers the full-batch gradient at $\boldsymbol{\theta}$. Here, $\hat{y}(f)$ denotes the prediction function which is the sigmoid function for binary logistic regression, that is, $\hat{y}(f) = \sigma(f) = 1/(1 + \exp(-f))$. The result shows that the optimal memory size is equal to K_t^* and perfect gradient recovery is possible by simply comparing K_t^* predictions at old and new models. This can be extremely cheap compared to the full batch gradient for long data streams whose intrinsic dimensionality is much smaller.

The main issue with the method is that computing $w_{k|t}^*$ for each $\boldsymbol{\theta}$ is infeasible in practice because it requires access to all of the past data. Specifically, the optimal value is given by

$$w_{k|t}^* = \frac{s_{k|t}^* (\mathbf{v}_{k|t}^*)^\top \mathbf{d}_x}{\sigma(\mathbf{u}_{k|t}^\top \boldsymbol{\theta}) - \sigma(\mathbf{u}_{k|t}^\top \boldsymbol{\theta}_t)} \quad (9)$$

which require computation of the vector \mathbf{d}_x whose length is equal to the data size $|\mathcal{D}_{1:t}|$, with the j 'th entry is equal to $\sigma(\phi_j^\top \boldsymbol{\theta}) - \sigma(\phi_j^\top \boldsymbol{\theta}_t)$. Since we do not have access to old features ϕ_j , it is impossible to find the optimal $w_{k|t}^*$ for all $\boldsymbol{\theta}$ values. In what follows, we propose a practical method to estimate such compact memory for continual logistic regression, for both binary and multi-class cases. We do not aim to exactly obtain the optimal memory but still hope to keep the memory size small enough so that it is not much larger than the rank of the feature matrix. Our method uses Hessian matching which is related to other theoretical works [Li et al., 2023, Ding et al., 2024, Li et al., 2025].

3 Compact Memory for K-prior

We now present a practical alternative to estimate the optimal memory for continual logistic regression. Throughout, we assume a quadratic regularizer $\frac{1}{2}\delta_t\|\boldsymbol{\theta}\|^2$ needed for training at task t ; the method can easily handle other regularizers as well. Motivated by Eq. 8, we propose to define the K-prior by using a set of *unit-norm* memory vectors $\mathbf{u}_{k|t}$ and their weights $w_{k|t}$, as shown below:

$$\mathcal{K}_t(\boldsymbol{\theta}; \mathbf{U}_t, \mathbf{w}_t) = \frac{1}{2}\delta_t\|\boldsymbol{\theta} - \boldsymbol{\theta}_t\|^2 + \sum_{k=1}^{K_t} w_{k|t} \mathcal{L}\left(\hat{y}(\mathbf{u}_{k|t}^\top \boldsymbol{\theta}_t), \hat{y}(\mathbf{u}_{k|t}^\top \boldsymbol{\theta})\right), \quad (10)$$

The set of memory and weight vectors are respectively defined as follows,

$$\mathbf{U}_t = (\mathbf{u}_{1|t} \ \mathbf{u}_{2|t} \ \dots \ \mathbf{u}_{K_t|t}) \quad \text{and} \quad \mathbf{w}_t = (w_{1|t} \ w_{2|t} \ \dots \ w_{K_t|t}), \quad (11)$$

and we denote by \mathbf{W}_t the diagonal matrix whose diagonal is the vector \mathbf{w}_t . Clearly, a fixed \mathbf{w}_t will not yield the optimal K-prior but we still hope that it will make the memory more compact. To estimate the memory and weights, we start with an initial value of $(\mathbf{U}_0, \mathbf{w}_0)$ at $t = 0$ and use the following iterative procedure (illustrated in Fig. 1),

1. Estimate $\boldsymbol{\theta}_{t+1}$ by training over $\bar{\ell}_{t+1}(\boldsymbol{\theta}; \mathcal{D}_{t+1}) + \mathcal{K}_t(\boldsymbol{\theta}; \mathbf{U}_t, \mathbf{w}_t)$.
2. Estimate $(\mathbf{U}_{t+1}, \mathbf{w}_{t+1})$ by using Hessian matching (with PPCA).

The first step is simply the standard K-prior training as in Eq. 6. Next, we motivate the second step on a linear regression problem and then present an extension for logistic regression.

3.1 Compact Memory for Linear Regression

We consider the following linear regression problem and show that estimating the second step can be realized via Hessian matching,

$$\sum_{j=0}^t \bar{\ell}_j(\boldsymbol{\theta}; \mathcal{D}_j) = \frac{1}{2}\delta_t\|\boldsymbol{\theta}\|^2 + \sum_{j=1}^t \sum_{i \in \mathcal{D}_j} \mathcal{L}\left(y_i, \hat{y}(\phi_i^\top \boldsymbol{\theta})\right), \quad \text{where } \mathcal{L}(y, \hat{y}) = \frac{1}{2}(y - \hat{y})^2. \quad (12)$$

Here, we denote the quadratic regularizer $\frac{1}{2}\delta_t\|\theta\|^2$ by $\bar{\ell}(\theta; \mathcal{D}_0)$. For this problem, the K-prior can perfectly recover the joint loss if memory is chosen optimally, as stated in the following theorem.

Theorem 1 *For the problem in Eq. 12, the K-prior shown in Eq. 10 is equivalent to the original loss and takes a quadratic form if we set $\theta_t \leftarrow \theta_t^*$, $\mathbf{U}_t \leftarrow \mathbf{U}_t^*$ and $\mathbf{W}_t \leftarrow \mathbf{S}_t^*$, that is, we have*

$$\sum_{j=0}^t \bar{\ell}_j(\theta; \mathcal{D}_j) = \mathcal{K}_t(\theta; \mathbf{U}_t, \mathbf{w}_t) = \frac{1}{2}(\theta - \theta_t)^\top \mathbf{H}(\theta_t)(\theta - \theta_t), \quad (13)$$

where $\mathbf{H}(\theta_t) = \Phi_{1:t} \Phi_{1:t}^\top + \delta_t \mathbf{I}$ is the Hessian of the objective in Eq. 12.

A proof is included in App. A.1.

This result gives a clue on how to estimate the next $(\mathbf{U}_{t+1}, \mathbf{w}_{t+1})$. Essentially, if $\theta_{t+1} \leftarrow \theta_{t+1}^*$ as well, then we should choose $(\mathbf{U}_{t+1}, \mathbf{w}_{t+1})$ such that the following holds for all θ ,

$$\mathcal{K}_{t+1}(\theta; \mathbf{U}_{t+1}, \mathbf{w}_{t+1}) = \bar{\ell}_{t+1}(\theta; \mathcal{D}_{t+1}) + \mathcal{K}_t(\theta; \mathbf{U}_t, \mathbf{w}_t). \quad (14)$$

Such a choice will ensure that the batch training loss for tasks 1 to $t+1$ is perfectly reconstructed with the new K-prior \mathcal{K}_{t+1} . For linear regression, this condition is satisfied by using the second-order optimality condition, obtained by taking the second derivative of both sides at θ_{t+1} . This is because the Hessian is independent of θ and Hessian matching yields

$$\mathbf{U}_{t+1} \mathbf{W}_{t+1} \mathbf{U}_{t+1}^\top + \epsilon_{t+1} \mathbf{I} = \Phi_{t+1} \Phi_{t+1}^\top + \mathbf{U}_t \mathbf{W}_t \mathbf{U}_t^\top, \quad (15)$$

where $\epsilon_{t+1} = (\delta_{t+1} - \delta_t)$. We note that this is not possible by using the first-order optimality condition because gradients are of the same size as θ , which is not enough to estimate a (larger) \mathbf{U}_t . In contrast, the condition above is sufficient and is just another way to formulate an online SVD procedure. Essentially, we can concatenate $(\Phi_{t+1}, \mathbf{U}_t \mathbf{W}_t^{1/2})$ and apply SVD to it to obtain \mathbf{U}_{t+1} and \mathbf{w}_{t+1} . The last term ϵ_{t+1} represents the error made in this process which can be driven to zero by choosing K_{t+1} appropriately. SVD can however be numerically unstable and we will use an alternative based on PPCA, which is easier to implement and also have an intuitive interpretation.

3.2 Hessian Matching via Probabilistic PCA (PPCA)

Hessian matching can be formulated as Probabilistic PCA [Tipping and Bishop, 1999a] and conveniently solved using the Expectation Maximization (EM) algorithm. Essentially, we aim to find \mathbf{U}_{t+1} whose columns can accurately predict the columns of Φ_{t+1} and \mathbf{U}_t . More formally, we define the following two matrices,

$$\mathbf{T} \leftarrow \sqrt{N}(\Phi_{t+1}, \mathbf{U}_t \mathbf{W}_t^{1/2}), \quad (16)$$

where $N \leftarrow K_t + |\mathcal{D}_{t+1}|$. Then, we use the following PPCA model to predict the columns \mathbf{t}_i of \mathbf{T} ,

$$\mathbf{t}_i = \mathbf{U}_{t+1} \mathbf{W}_{t+1}^{1/2} \mathbf{z}_i + \mathbf{e}_i, \quad \text{where } \mathbf{z}_i \sim \mathcal{N}(0, \mathbf{I}) \text{ and } \mathbf{e}_i \sim \mathcal{N}(0, \epsilon_{t+1} \mathbf{I}). \quad (17)$$

We now show that maximum-likelihood estimation on this model can find $(\mathbf{U}_{t+1}, \mathbf{w}_{t+1})$ that solve Eq. 15. As shown by Tipping and Bishop [1999a, Eq. 4], the log marginal-likelihood of this model is obtained by noting that \mathbf{t}_i follows a Gaussian distribution too, which gives (details in App. A.2)

$$\log p(\mathbf{T} | \mathbf{U}_{t+1}, \mathbf{w}_{t+1}) = -\frac{1}{2}N \left[\log |\mathbf{C}| + \text{Tr} \left(\mathbf{C}^{-1} \mathbf{T} \mathbf{T}^\top / N \right) \right] + \text{cst.} \quad (18)$$

where $\mathbf{C} = \mathbf{U}_{t+1} \mathbf{W}_{t+1} \mathbf{U}_{t+1}^\top + \epsilon_{t+1} \mathbf{I}$. Then, taking the derivative and setting it to 0, we can show that the optimality condition is to set $\mathbf{C} = \mathbf{T} \mathbf{T}^\top / N$ which is equivalent to Eq. 15; a derivation is included in App. A.2. Similarly to online SVD, maximum likelihood over PPCA also performs Hessian matching. PPCA also enables us to estimate ϵ_{t+1} , but for simplicity we fix it to a constant value (denoted by ϵ from now onward).

The main advantage of this formulation is that it leads to an easy-to-implement EM algorithm. Essentially, in the E-step, we find the posterior over \mathbf{z}_i , then in M-step, we update $\tilde{\mathbf{U}}$. The two steps can be conveniently written in just one line [Tipping and Bishop, 1999a, Eq. 29]. This is obtained by denoting $\tilde{\mathbf{U}} \leftarrow \mathbf{U}_{t+1} \mathbf{W}_{t+1}^{1/2}$ and updating it as follows:

$$\tilde{\mathbf{U}} \leftarrow \tilde{\mathbf{S}} \tilde{\mathbf{U}} (\epsilon \mathbf{I} + \mathbf{M}^{-1} \tilde{\mathbf{U}}^\top \tilde{\mathbf{S}} \tilde{\mathbf{U}})^{-1}, \quad \text{where } \mathbf{M} = \tilde{\mathbf{U}}^\top \tilde{\mathbf{U}} + \epsilon \mathbf{I} \quad \text{and} \quad \mathbf{S} = \mathbf{T} \mathbf{T}^\top / N. \quad (19)$$

Algorithm 1: Hessian Matching by PPCA

Require: Φ_{t+1} , \mathbf{U}_t , \mathbf{w}_t and ϵ

- 1: $\mathbf{W} \leftarrow \text{Diag}(\mathbf{w}_t)$ and $\tilde{\mathbf{U}} \leftarrow \mathbf{U}_t \mathbf{W}^{1/2}$
- 2:
- 3: $\mathbf{T} \leftarrow (\Phi_{t+1}, \mathbf{U}_t \mathbf{W}^{1/2})$
- 4: $\mathbf{S} \leftarrow \mathbf{T} \mathbf{T}^\top$
- 5: **while** not converged **do**
- 6:
- 7: $\mathbf{M} \leftarrow \tilde{\mathbf{U}}^\top \tilde{\mathbf{U}} + \epsilon \mathbf{I}$
- 8: $\tilde{\mathbf{U}} \leftarrow \mathbf{S} \tilde{\mathbf{U}} (\epsilon \mathbf{I} + \mathbf{M}^{-1} \tilde{\mathbf{U}}^\top \mathbf{S} \tilde{\mathbf{U}})^{-1}$
- 9:
- 10: **end while**
- 11: $\mathbf{w} \leftarrow \text{diag}(\tilde{\mathbf{U}}^\top \tilde{\mathbf{U}})$ and $\mathbf{W} \leftarrow \text{Diag}(\mathbf{w})$
- 12: $\mathbf{U} \leftarrow \tilde{\mathbf{U}} \mathbf{W}^{-1/2}$
- 13: **return** $\mathbf{U}_{t+1} \leftarrow \mathbf{U}$ and $\mathbf{w}_{t+1} \leftarrow \mathbf{w}$

Algorithm 2: Extension for Logistic Regression

Require: Φ_{t+1} , \mathbf{U}_t , \mathbf{w}_t , ϵ , and θ_{t+1}

- 1: $\mathbf{W} \leftarrow \text{Diag}(\mathbf{w}_t)$ and $\mathbf{U} \leftarrow \mathbf{U}_t$
- 2: $\lambda_1 \leftarrow \hat{y}'(\Phi_{t+1}^\top \theta_{t+1})$ and $\lambda_2 \leftarrow \hat{y}'(\mathbf{U}_t^\top \theta_{t+1})$
- 3: $\mathbf{T} \leftarrow (\Phi_{t+1} \text{Diag}(\lambda_1)^{1/2}, \mathbf{U}_t \mathbf{W}^{1/2} \lambda_2^{1/2})$
- 4: $\mathbf{S} \leftarrow \mathbf{T} \mathbf{T}^\top$
- 5: **while** not converged **do**
- 6: $\lambda \leftarrow \hat{y}'(\mathbf{U}^\top \theta_{t+1})$ and $\tilde{\mathbf{U}} \leftarrow \mathbf{U} (\mathbf{W} \lambda)^{1/2}$
- 7: $\mathbf{M} \leftarrow \tilde{\mathbf{U}}^\top \tilde{\mathbf{U}} + \epsilon \mathbf{I}$
- 8: $\tilde{\mathbf{U}} \leftarrow \mathbf{S} \tilde{\mathbf{U}} (\epsilon \mathbf{I} + \mathbf{M}^{-1} \tilde{\mathbf{U}}^\top \mathbf{S} \tilde{\mathbf{U}})^{-1}$
- 9: $\tilde{\mathbf{U}} \leftarrow \tilde{\mathbf{U}} \lambda^{-1/2}$
- 10: $\mathbf{w} \leftarrow \text{diag}(\tilde{\mathbf{U}}^\top \tilde{\mathbf{U}})$ and $\mathbf{W} \leftarrow \text{Diag}(\mathbf{w})$
- 11: $\mathbf{U} \leftarrow \tilde{\mathbf{U}} \mathbf{W}^{-1/2}$
- 12: **end while**
- 13: **return** $\mathbf{U}_{t+1} \leftarrow \mathbf{U}$ and $\mathbf{w}_{t+1} \leftarrow \mathbf{w}$

Figure 2: The left side shows a Hessian-matching algorithm for linear regression obtained using EM for PPCA. On the right, an extension for logistic regression is shown where differences to the regression case highlighted in red. The main differences are in line 2, 3, 6, and 9, and they all mostly due to the inclusion of terms that contain $\hat{y}'(f)$. For logistic regression, $\hat{y}'(f) = \sigma(f)[1 - \sigma(f)]$. When operated on a vector \mathbf{f} , $\hat{y}'(\mathbf{f})$ returns a vector of $\hat{y}'(f_i)$. $\text{Diag}(\mathbf{w})$ denotes a diagonal matrix with vector \mathbf{w} as the diagonal, while $\text{diag}(\mathbf{W})$ returns back the diagonal vector of \mathbf{W} .

Derivation is included in App. A.2 and an algorithm to implement this procedure is outlined in Alg. 1, where in lines 11-12, we normalize columns of $\tilde{\mathbf{U}}$ to obtain $(\mathbf{U}_{t+1}, \mathbf{w}_{t+1})$. The algorithm assumes that $K_{t+1} = K_t$, but if memory size is increased, then we need just one additional step to initialize the additional vectors (we can do this in line 1). In practice, we use a subset of Φ_{t+1} to initialize the new memory vectors. The EM procedure implements Hessian matching by essentially finding new memory vectors that can predict old memories as well as the new features.

3.3 An Extension for Binary Logistic Regression

We now show an extension for binary logistic regression. The procedure also works for other generalized linear models but we omit it because the derivation is straightforward. We will however briefly discuss an extension to multi-class afterward.

For binary logistic regression, aiming for a recursion similar to Eq. 14 is challenging. As discussed earlier, this is because computing the optimal $w_{k|t}$ is infeasible in practice. To simplify the estimation, we relax this requirement and aim for Hessian matching at θ_{t+1} . That is, we reformulate the search for $(\mathbf{U}_{t+1}, \mathbf{w}_{t+1})$ as the following Hessian-matching problem at θ_{t+1} ,

$$\nabla^2 \mathcal{K}_{t+1}(\theta_{t+1}; \mathbf{U}_{t+1}, \mathbf{w}_{t+1}) = \nabla^2 \bar{\ell}_{t+1}(\theta_{t+1}; \mathcal{D}_{t+1}) + \nabla^2 \mathcal{K}_t(\theta_{t+1}; \mathbf{U}_t, \mathbf{w}_t). \quad (20)$$

This condition leads to an equation shown below which takes a form similar to Eq. 15 obtained for the linear regression case. A derivation is given in App. A.3, where we show that the only difference is in the diagonal matrices which are defined differently:

$$\mathbf{U}_{t+1} \tilde{\mathbf{W}}_{t+1} \mathbf{U}_{t+1}^\top + \epsilon_{t+1} \mathbf{I} = \Phi_{t+1} \mathbf{B}_{t+1} \Phi_{t+1}^\top + \mathbf{U}_t \tilde{\mathbf{W}}_t \mathbf{U}_t^\top, \quad (21)$$

where $\tilde{\mathbf{W}}_{t+1}$, $\tilde{\mathbf{W}}_t$, and \mathbf{B}_{t+1} are the diagonal matrices defined as follows:

$$\tilde{\mathbf{W}}_{t+1} = \mathbf{W}_{t+1} \hat{y}'(\mathbf{U}_{t+1}^\top \theta_{t+1}), \quad \tilde{\mathbf{W}}_t = \mathbf{W}_t \hat{y}'(\mathbf{U}_t^\top \theta_{t+1}), \quad \mathbf{B}_{t+1} = \text{Diag}[\hat{y}'(\Phi_{t+1}^\top \theta_{t+1})]. \quad (22)$$

Here, the function $\hat{y}'(f)$ denotes the first derivative of $\hat{y}(f)$ with respect to f . For binary logistic regression, $\hat{y}(f) = \sigma(f)$, therefore $\hat{y}'(f) = \sigma(f)(1 - \sigma(f))$. When applied to a vector \mathbf{f} , $\hat{y}'(\mathbf{f})$ returns a vector of $\hat{y}'(f_j)$, which is the case for all the quantities used above. In last expression $\text{Diag}(\mathbf{f})$ forms a diagonal matrix whose diagonal is the vector \mathbf{f} .

The new Hessian matching equation can also be solved using an algorithm similar to [Alg. 1](#), shown in [Alg. 2](#). We will now briefly describe how to derive the algorithm. First, instead of using [Eq. 16](#), we redefine \mathbf{T} as shown below where we include some vectors computed using the function $\hat{y}(\cdot)$,

$$\mathbf{T} \leftarrow \sqrt{N}(\Phi_{t+1}\text{Diag}(\lambda_1)^{1/2}, \mathbf{U}_t\mathbf{W}_t^{1/2}\lambda_2^{1/2}), \quad (23)$$

where we use $\lambda_1 \leftarrow \hat{y}'(\Phi_{t+1}^\top \theta_{t+1})$ and $\lambda_2 \leftarrow \hat{y}'(\mathbf{U}_t^\top \theta_{t+1})$. With this change, $\mathbf{T}\mathbf{T}^\top/N$ is equal to the matrix in the right hand side of [Eq. 20](#). This is done in line 2 and 3 of [Alg. 2](#). The next change is in the update of \mathbf{U}_{t+1} . Essentially, we redefine

$$\tilde{\mathbf{U}}_{t+1} \leftarrow \mathbf{U}_{t+1}\mathbf{W}_{t+1}^{1/2}\lambda^{1/2} \quad (24)$$

where $\lambda \leftarrow \hat{y}'(\mathbf{U}_{t+1}^\top \theta_{t+1})$. With this change, the left hand side in [Eq. 20](#) becomes $\tilde{\mathbf{U}}\tilde{\mathbf{U}}^\top$, and then we can apply the update shown in [Eq. 19](#). This is done in line 6-8. Finally, because we need to recompute λ every time we update $\tilde{\mathbf{U}}$, we regularly extract $(\mathbf{U}_{t+1}, \mathbf{w}_{t+1})$ from $\tilde{\mathbf{U}}_{t+1}$, which is done in line 9-12. One minor change is to initialize the procedure in line 1.

The computational cost of the EM algorithm is dominated by the inversion in line 8 of a square matrix of size K_{t+1} . Therefore, the overall complexity is in $\mathcal{O}(IK_{t+1}^3)$ where I is the number of iterations. For small K_{t+1} and I , this cost is manageable and does not add a huge overhead to overall training.

3.4 Extensions for Multi-Class Logistic Regression and Other Generalized Linear Models

[Alg. 2](#) can be easily extended to estimate compact memory for other generalized linear models. The main change required is to appropriately define the function $\hat{y}'(f)$. We demonstrate this for multi-class logistic regression with number of classes C . For this case, we define a parameter vector $\theta^{(c)}$ for each class c , giving rise to the matrix $\Theta = (\theta^{(1)} \dots \theta^{(C)})^\top$. The linear predictor for a feature ϕ (of length P) is defined as $\mathbf{f} = \Theta\phi$ and is of length C . Given such a linear predictor, the prediction function and its derivatives are defined through the softmax function as shown below,

$$\hat{y}(\mathbf{f}) = \mathbf{p} \text{ and } \hat{y}'(\mathbf{f}) = \text{Diag}(\mathbf{p}) - \mathbf{p}\mathbf{p}^\top, \text{ where } c\text{'th entry of } \mathbf{p} \text{ is } p^{(c)} = \frac{\exp(f^{(c)})}{\sum_{c'=1}^C \exp(f^{(c')})}, \quad (25)$$

which are vector and matrix of size P , respectively. The gradient and Hessian are given by

$$\frac{\partial \mathcal{L}(\mathbf{y}, \hat{y}(\mathbf{f}))}{\partial \theta^{(c)}} = [\hat{y}(f^{(c)}) - y^{(c)}]\phi, \quad \frac{\partial^2 \mathcal{L}(\mathbf{y}, \hat{y}(\mathbf{f}))}{\partial \theta^{(c)} \partial \theta^{(c')\top}} = [\hat{y}'(\mathbf{f})]^{(c,c')} \phi \phi^\top,$$

where $[\hat{y}'(\mathbf{f})]^{(c,c')}$ denotes the entry (c, c') of the matrix. As a result, the size of the Hessian of the loss $\mathcal{L}(\mathbf{y}, \hat{y}(\mathbf{f}))$ with respect to (vectorized) Θ is a $PC \times PC$ matrix where P is the length of each $\theta^{(c)}$. Since a $P \times P$ matrix is sufficient to estimate the memory vectors of size $P \times K_{t+1}$, we choose to perform Hessian matching over the sum $\sum_{c=1}^C \frac{\partial^2 \mathcal{L}}{\partial \theta^{(c)} \partial \theta^{(c)\top}}$, that is, we use the following,

$$\sum_{c=1}^C \nabla^2 \mathcal{K}_{t+1}(\theta_{t+1}^{(c)}; \mathbf{U}_{t+1}, \mathbf{w}_{t+1}) = \sum_{c=1}^C \left[\nabla^2 \bar{\ell}_{t+1}(\theta_{t+1}^{(c)}; \mathcal{D}_{t+1}) + \nabla^2 \mathcal{K}_t(\theta_{t+1}^{(c)}; \mathbf{U}_t, \mathbf{w}_t) \right]. \quad (26)$$

This condition ignores the cross-derivatives between all pairs $c \neq c'$, but the Hessian matching takes a similar form to [Eq. 21](#). Essentially, we can push the sum with respect to c inside because the only quantity that depends on c is $\hat{y}(f^{(c)})$. Due to this change, we need to redefine the diagonal entries of the matrices $\tilde{\mathbf{W}}_{t+1}$, $\tilde{\mathbf{W}}_t$, and \mathbf{B}_{t+1} by using the trace of $\hat{y}'(\mathbf{f})$, as shown below (details in [App. A.4](#)):

$$\tilde{\mathbf{W}}_{t+1}^{(kk)} = w_{k|t+1} \text{Tr}[\hat{y}'(\Theta_{t+1} \mathbf{u}_{k|t+1})], \quad \tilde{\mathbf{W}}_t^{(kk)} = w_{k|t} \text{Tr}[\hat{y}'(\Theta_{t+1} \mathbf{u}_{k|t})], \quad (27)$$

$$\mathbf{B}_{t+1}^{(jj)} = \text{Tr}[\hat{y}'(\Theta_{t+1} \phi_j)],$$

where k runs from 1 to K_t (or K_{t+1}) and j runs from 1 to $|\mathcal{D}_{1+t}|$. The trace function is denoted by $\text{Tr}(\hat{y}'(\mathbf{f})) = \sum_c p^{(c)}(1 - p^{(c)})$ which takes a similar form to the binary case. Essentially, a large value of this quantity indicates that the corresponding feature is important for at least one class. To improve numerical stability, we clip the vector \mathbf{p} away from 1 or 0 by a small amount (we use 10^{-4}). Overall, this example demonstrates how to extend our approach to other generalized linear models.

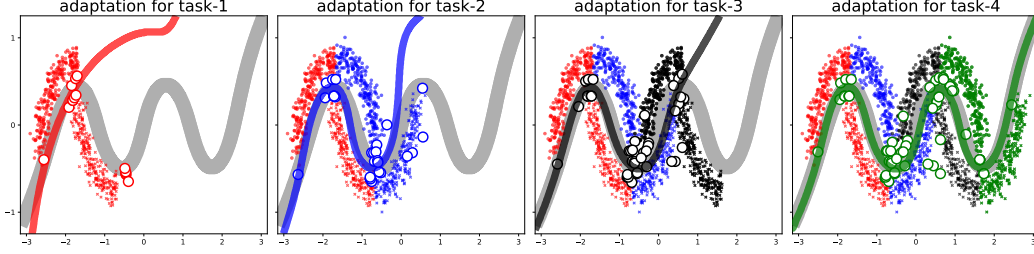


Figure 3: Binary logistic regression on a toy ‘four-moon’ datasets with four tasks (red \rightarrow blue \rightarrow black \rightarrow green). The gray line shows the batch training, while our compact-memory method’s boundary are shown with colors. We see that estimated boundary closely tracks the batch solution and ultimately recovers it at the end of training. We also show with circles the points in the input space that are closed to the memories in terms of the loss gradient.

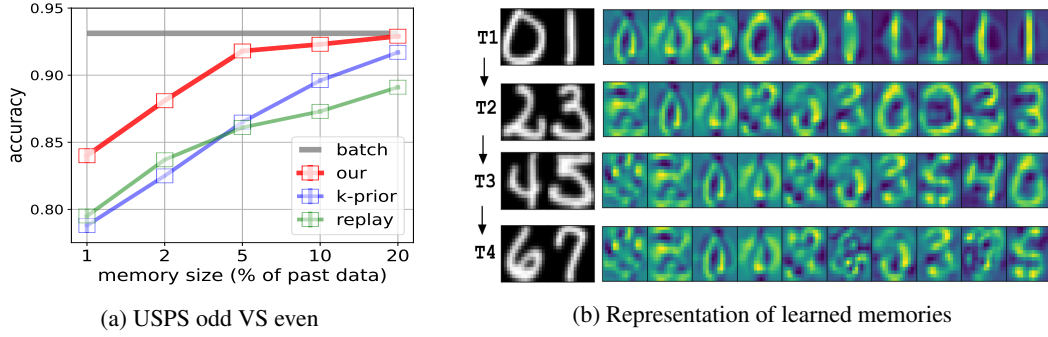


Figure 4: Panel (a) shows results for binary classification on USPS-odd-vs-even dataset. For each $\mathbf{x} \in \mathbb{R}^{256}$, the 1-order polynomial feature-map is used, that is, $\phi(\mathbf{x}) = [1, \mathbf{x}] \in \mathbb{R}^{257}$ is used. Our method clearly beats both replay and K-prior (no learned memories) and obtains performance close to batch. Panel (b) visualizes the learned memories when using memory size of 1%. Each row shows the learned memory (as images) sorted according to their weights $w_{k|t}$ (left to right in descending order). We clearly see that new features emerge as new tasks arrive.

4 Experimental Results

We show the following results: (i) multi-output linear regression for sanity check, (ii) two binary logistic regression on toy data and USPS dataset, and (iii) multi-class logistic regression on four datasets based on CIFAR-10, CIFAR-100, TinyImageNet-200, and ImageNet-100. The multi-output regression result is included in [App. B.1](#) where we compare to the vanilla SVD and show that our method is numerically more robust. The rest of the results are described in the next section. More details of the experiments are also included in [App. B](#).

4.1 Binary Logistic Regression

We show that for continual logistic regression our method improves over the replay and vanilla K-prior methods. We start with the toy example on the ‘four-moon’ dataset and then show results for the USPS dataset. Both results follow the experimental setting used by [Khan and Swaroop \[2021\]](#).

Four-moon dataset. We split the four-moon dataset into four binary tasks and perform continual logistic regression over them. The training set of each task consists of 500 data points and we test over all inputs obtained on a 2-D grid $(-3.2, 3.2) \times (-1.2 \times 1.2)$ in the input space (a total of 158,632). We use a polynomial feature map of degree 5. The memory size is set to the half of feature dimensions per task and increased in this fashion with every new task. [Fig. 3](#) shows the changes in the decision boundary as the model trains on tasks, where we see that the classifier closely follows the decision boundary of the batch training (shown in gray), ultimately recovering them after 4 tasks.

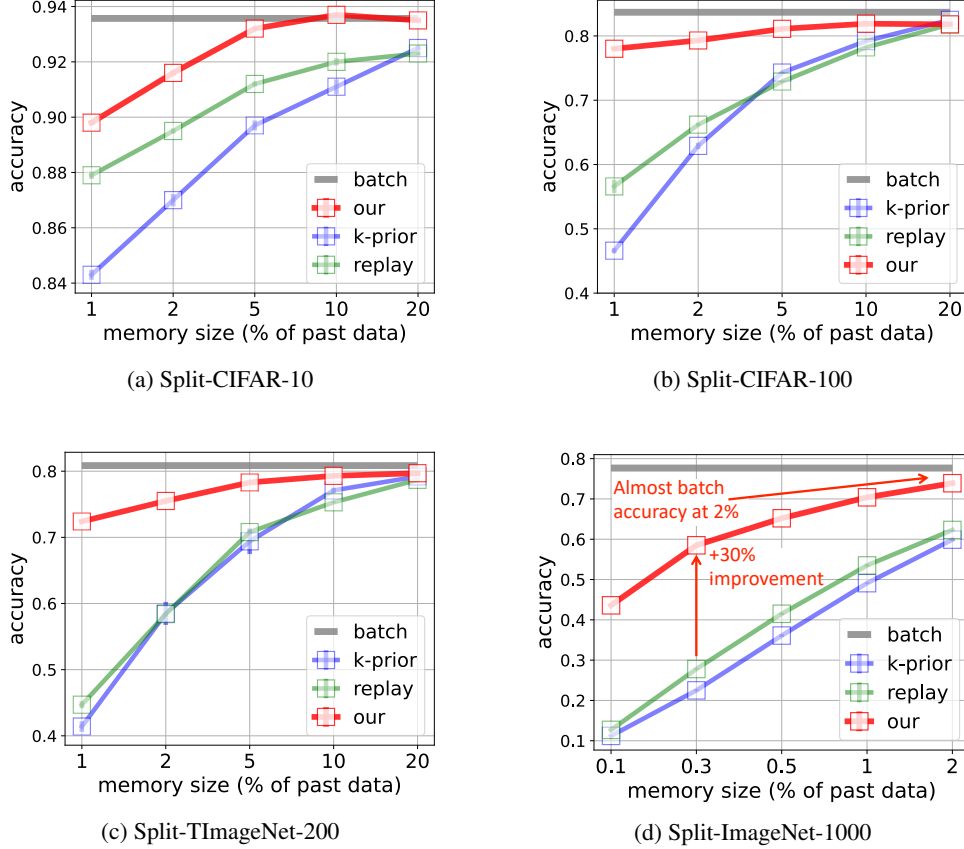


Figure 5: Results for multi-class logistic regression. For panel (a), we use features extracted using a pre-trained ViT-B/32 and the rest use features of a pre-trained ViT-L/14. Similarly to binary classification, our method get much better accuracy compared to replay and K-prior for the same memory size. For instance, on Split-ImageNet-1000, we get 30% improvement over replay when using memory size equivalent to 0.3% of the data size. With 2% memory, we obtain 74% accuracy which is close to the batch accuracy of 77.6% on this dataset.

To understand the nature of the newly learned memories, we also plot the data examples that are closest to the learned memories (shown with circles in Fig. 3). To be precise, we find examples \mathbf{x}_* in the input space whose gradient is closest to a memory vector, that is, for a given $\mathbf{u}_{k|t}$, we look for \mathbf{x} with the smallest $\|\nabla_{\theta} \mathcal{L}(y, \hat{y}(f_{\theta}(\mathbf{u}_{k|t}))) - \nabla_{\theta} \mathcal{L}(y, \hat{y}(f_{\theta}(\mathbf{x})))\|_2$ at $\theta = \theta_t$. We see that learned memories cover areas in the input space close to the decision boundary. This confirms that the memories are a reasonable representation of the decision boundary.

USPS odd vs even datasets. The USPS dataset is a 16×16 image dataset of digits from 0 to 9. We relabel each digit based on whether it is even or odd and consider a continual logistic regression with 5 task sequences given as $(0, 1) \rightarrow (2, 3) \rightarrow (4, 5) \rightarrow (6, 7) \rightarrow (8, 9)$. The training set of each task consists of 1000 data points, and the test set of each task consists of 300 data points. We use degree-1 polynomial feature-map yielding 256-dimensional features.

We consider the following baselines: K-prior [Khan and Swaroop, 2021] and experience replay [Rolnick et al., 2019] that store partial datasets of past tasks as memory. The replay set of K-prior and experience replay are initialized by random data subsets as done in Daxberger et al. [2023]. We also compare to the batch training.

Fig. 4a shows the averaged accuracies on the test set over five tasks when the varying memory sizes are considered. For each experiment we use five different random seeds. We plot results for memory sizes equivalent to 1, 2, and 5% of dataset for memory. The result shows that our method outperforms other baselines significantly when using small memory sizes. Fig. 4b shows the visualization of the

ten trained memories when memory size is set to 1% of the data. The memory vectors are sorted according to their weights $w_{k|t}$ (left to right in descending order) and visualized in an image form. With new tasks arriving, memories with new features are learned.

4.2 Multi-Class Logistic Regression using Pre-Trained Neural Network Features

We now show results following those done by Carta et al. [2023]. We use the feature map $\phi(x)$ of Vision Transformer (Vit) [Dosovitskiy et al., 2021] which is pre-trained using CLIP (available at <https://github.com/openai/CLIP>). These are known to yield effective features for classifying various image datasets [Radford et al., 2021]. We construct the features $\{\phi(x); (x, y) \in \mathcal{D}_t\}$ for t -th task \mathcal{D}_t while freezing the parameters of the feature extractor and then use them for multi-class classification with logistic regression. We use the same baselines as the previous experiment.

We compare the performance on the following benchmarks:

1. Split-CIFAR-10 is a sequence of 5 tasks constructed by dividing 50,000 examples of CIFAR-10 into non-overlapping subsets. Each task contains 2 consecutive classes.
2. Split-CIFAR-100 is a sequence of 20 tasks constructed by dividing 50,000 examples of CIFAR-100 into non-overlapping subsets. Each task contains 5 consecutive classes.
3. Split-TinyImageNet-200 is a sequence of 20 tasks constructed by dividing 100,000 examples of TinyImageNet-200 into non-overlapping subsets. Each task contains 10 consecutive classes.
4. Split-ImageNet-1000 is a sequence of 10 tasks constructed by dividing 1,281,167 examples of ImageNet-1000 into non-overlapping subsets. Each task contains 100 consecutive classes.

Results. Fig. 5 shows the test accuracy on each benchmark over 5 random seeds. In each figure, the x -axis shows the memory size and the y -axis shows the average accuracy over all tasks. Notably, when only 1% of the dataset is used for memory, our method significantly outperforms both replay and K-prior that use randomly selected memory. For instance, on Split-ImageNet-1000, we get 30% improvement by just using 0.3% memory size, and obtain close to batch performance by just using 2% of the data (74% vs 77.6% obtained by batch). These results clearly show the memory efficiency of our method.

Fig. 6 illustrates the computational overhead of our method compared to experience replay. Under the same setting as the Split-ImageNet-1000 experiment, we consider 5 and 10 EM iterations per task; the result of 10 iterations are reported in Fig. 5. The ratio of running times, ours to replay, is reported to directly compare computational overhead. The result shows that the computational overhead of our method increases only marginally when using a smaller amount of memory. We believe that this level of computational overhead is acceptable for learning compact memory, which is the primary target of our research.

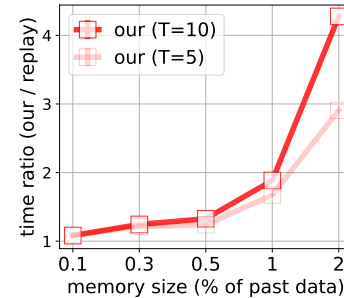


Figure 6: Running time.

5 Discussion

As large pre-trained neural networks show remarkable performance, adaptation of these models to new environments is becoming increasingly important. However, even in the case of continual learning with a shallow neural network, the performance tends to degrade due to catastrophic forgetting issues. To remedy this issue, models require storing a substantial memory as the learning progresses, which makes continual learning less practical.

In this work, we present a Hessian matching method to obtain compact memory for continual logistic regression. We demonstrate that, this compact memory, seeking for accurate gradient reconstructions of past tasks' losses, significantly boosts memory efficiency. We further show that the memory efficiency holds even when the compact memory is used jointly with the pre-trained neural network as a feature extractor. Although our algorithm is currently limited to the use of only the last-layer of a neural network with a frozen feature extractor, to ensure the principle of gradient reconstruction, we expect that this simple solution opens a new path to finding the compact memory for large-scale deep neural networks such as a foundation model, and that this compact memory enables these models to continually adapt to new tasks in a memory-efficient way.

Acknowledgments and Disclosure of Funding

Y. J., T. M., and M. E. K. are supported by the Bayes duality project, JST CREST Grant Number JPMJCR2112. H. L. is supported by the Institute of Information & Communications Technology Planning & Evaluation (IITP) grant funded by the Korea government (MSIT) (No.RS-2025-02219317, AI Star Fellowship (Kookmin University)). H. L. is also supported by the Institute of Information & Communications Technology Planning & Evaluation(IITP) grant funded by the Korea government(MSIT) (No.RS-2025-02263754, Human-Centric Embodied AI Agents with Autonomous Decision-Making).

References

- Mohammad Emtiyaz Khan and Siddharth Swaroop. Knowledge-adaptation priors. In *Advances in Neural Information Processing Systems (NeurIPS)*, 2021.
- Martial Mermillod, Aurélia Bugaïska, and Patrick Bonin. The stability-plasticity dilemma: Investigating the continuum from catastrophic forgetting to age-limited learning effects. *Frontiers in Psychology*, 4:504, 2013.
- Richard S Sutton. Two problems with backpropagation and other steepest-descent learning procedures for networks. In *Proceedings of the Annual Meeting of the Cognitive Science Society*, 1986.
- James Kirkpatrick, Razvan Pascanu, Neil Rabinowitz, Joel Veness, Guillaume Desjardins, Andrei A Rusu, Kieran Milan, John Quan, Tiago Ramalho, Agnieszka Grabska-Barwinska, Demis Hassabis, Claudia Clopath, Dharshan Kumaran, and Raia Hadsell. Overcoming catastrophic forgetting in neural networks. *Proceedings of the National Academy of Sciences (PNAS)*, 114(13):3521–3526, 2017.
- Zhizhong Li and Derek Hoiem. Learning without forgetting. *IEEE Transactions on Pattern Analysis and Machine Intelligence*, 40(12):2935–2947, 2017.
- Sang-Woo Lee, Jin-Hwa Kim, Jaehyun Jun, Jung-Woo Ha, and Byoung-Tak Zhang. Overcoming catastrophic forgetting by incremental moment matching. In *Advances in Neural Information Processing Systems (NeurIPS)*, 2017.
- Friedemann Zenke, Ben Poole, and Surya Ganguli. Continual learning through synaptic intelligence. In *International Conference on Machine Learning (ICML)*, 2017.
- Sayna Ebrahimi, Mohamed Elhoseiny, Trevor Darrell, and Marcus Rohrbach. Uncertainty-guided continual learning in Bayesian neural networks. In *International Conference on Learning Representations (ICLR)*, 2020.
- Hippolyt Ritter, Aleksandar Botev, and David Barber. Online structured Laplace approximations for overcoming catastrophic forgetting. In *Advances in Neural Information Processing Systems (NeurIPS)*, 2018.
- Cuong V Nguyen, Yingzhen Li, Thang D Bui, and Richard E Turner. Variational continual learning. In *International Conference on Learning Representations (ICLR)*, 2018.
- David Rolnick, Arun Ahuja, Jonathan Schwarz, Timothy Lillicrap, and Gregory Wayne. Experience replay for continual learning. 2019.
- David Lopez-Paz and Marc’Aurelio Ranzato. Gradient episodic memory for continual learning. In *Advances in Neural Information Processing Systems (NeurIPS)*, 2017.
- Arslan Chaudhry, Marc’Aurelio Ranzato, Marcus Rohrbach, and Mohamed Elhoseiny. Efficient lifelong learning with A-GEM. In *International Conference on Learning Representations (ICLR)*, 2019.
- Michalis K Titsias, Jonathan Schwarz, Alexander G de G Matthews, Razvan Pascanu, and Yee Whye Teh. Functional regularisation for continual learning with Gaussian processes. In *International Conference on Learning Representations (ICLR)*, 2020.

- Pietro Buzzega, Matteo Boschini, Angelo Porrello, Davide Abati, and Simone Calderara. Dark experience for general continual learning: a strong, simple baseline. In *Advances in Neural Information Processing Systems (NeurIPS)*, 2020.
- Pingbo Pan, Siddharth Swaroop, Alexander Immer, Runa Eschenhagen, Richard Turner, and Mohammad Emtiyaz Khan. Continual deep learning by functional regularisation of memorable past. In *Advances in Neural Information Processing Systems (NeurIPS)*, 2020.
- Aidan Scannell, Riccardo Mereu, Paul Chang, Ella Tamir, Joni Pajarinen, and Arno Solin. Function-space parameterization of neural networks for sequential learning. In *International Conference on Learning Representations (ICLR)*, 2024.
- Rahaf Aljundi, Min Lin, Baptiste Goujaud, and Yoshua Bengio. Gradient based sample selection for online continual learning. In *Advances in Neural Information Processing Systems (NeurIPS)*, 2019a.
- Jaehong Yoon, Divyam Madaan, Eunho Yang, and Sung Ju Hwang. Online coreset selection for rehearsal-based continual learning. In *International Conference on Learning Representations (ICLR)*, 2022.
- Rahaf Aljundi, Eugene Belilovsky, Tinne Tuytelaars, Laurent Charlin, Massimo Caccia, Min Lin, and Lucas Page-Caccia. Online continual learning with maximal interfered retrieval. In *Advances in Neural Information Processing Systems (NeurIPS)*, 2019b.
- Shengyang Sun, Daniele Calandriello, Huiyi Hu, Ang Li, and Michalis Titsias. Information-theoretic online memory selection for continual learning. In *International Conference on Learning Representations (ICLR)*, 2022.
- Zalán Borsos, Mojmir Mutny, and Andreas Krause. Coresets via bilevel optimization for continual learning and streaming. In *Advances in Neural Information Processing Systems (NeurIPS)*, 2020.
- Erik Daxberger, Siddharth Swaroop, Kazuki Osawa, Rio Yokota, Richard E Turner, José Miguel Hernández-Lobato, and Mohammad Emtiyaz Khan. Improving continual learning by accurate gradient reconstructions of the past. *Transact. Mach. Learn. Res. (TMLR)*, 2023.
- Michael E Tipping and Christopher M Bishop. Probabilistic principal component analysis. *J. R. Stat. Soc. Ser. B Methodol.*, 61(3):611–622, 1999a.
- Haoran Li, Jingfeng Wu, and Vladimir Braverman. Fixed design analysis of regularization-based continual learning. In *Conference on Lifelong Learning Agents (CoLLAs)*, 2023.
- Meng Ding, Kaiyi Ji, Di Wang, and Jinhui Xu. Understanding forgetting in continual learning with linear regression. In *International Conference on Machine Learning (ICML)*, 2024.
- Haoran Li, Jingfeng Wu, and Vladimir Braverman. Memory-statistics tradeoff in continual learning with structural regularization. *arXiv preprint arXiv:2504.04039*, 2025.
- Antonio Carta, Lorenzo Pellegrini, Andrea Cossu, Hamed Hemati, and Vincenzo Lomonaco. Avalanche: A PyTorch library for deep continual learning. *J. Mach. Learn. Res. (JMLR)*, 24(363):1–6, 2023.
- Alexey Dosovitskiy, Lucas Beyer, Alexander Kolesnikov, Dirk Weissenborn, Xiaohua Zhai, Thomas Unterthiner, Mostafa Dehghani, Matthias Minderer, Georg Heigold, Sylvain Gelly, Jakob Uszkoreit, and Neil Houlsby. An image is worth 16x16 words: Transformers for image recognition at scale. In *International Conference on Learning Representations (ICLR)*, 2021.
- Alec Radford, Jong Wook Kim, Chris Hallacy, Aditya Ramesh, Gabriel Goh, Sandhini Agarwal, Girish Sastry, Amanda Askell, Pamela Mishkin, Jack Clark, Gretchen Krueger, and Ilya Sutskever. Learning transferable visual models from natural language supervision. In *International Conference on Machine Learning (ICML)*, 2021.
- Michael E Tipping and Christopher M Bishop. Mixtures of probabilistic principal component analyzers. *Neural Comput.*, 11(2):443–482, 1999b.

A Method Details

A.1 Proof of Theorem 1

We first write the quadratic form by noting that $\Phi_{1:t}\Phi_{1:t}^\top = \mathbf{U}_t\mathbf{W}_t\mathbf{U}_t^\top$,

$$\begin{aligned}\mathcal{K}_t(\boldsymbol{\theta}; \mathbf{U}_t, \mathbf{W}_t) &= \frac{1}{2}\delta_t\|\boldsymbol{\theta} - \boldsymbol{\theta}_t\|^2 + \sum_{k=1}^{K_t} \frac{1}{2}w_{k|t} (\mathbf{u}_{k|t}^\top \boldsymbol{\theta}_t - \mathbf{u}_{k|t}^\top \boldsymbol{\theta})^2 \\ &= \frac{1}{2}(\boldsymbol{\theta} - \boldsymbol{\theta}_t)^\top \left(\delta_t \mathbf{I} + \mathbf{U}_t \mathbf{W}_t \mathbf{U}_t^\top \right) (\boldsymbol{\theta} - \boldsymbol{\theta}_t) \\ &= \frac{1}{2}(\boldsymbol{\theta} - \boldsymbol{\theta}_t)^\top \left(\delta_t \mathbf{I} + \Phi_{1:t} \Phi_{1:t}^\top \right) (\boldsymbol{\theta} - \boldsymbol{\theta}_t) \\ &= \frac{1}{2}(\boldsymbol{\theta} - \boldsymbol{\theta}_t)^\top \mathbf{H}(\boldsymbol{\theta}_t) (\boldsymbol{\theta} - \boldsymbol{\theta}_t)\end{aligned}\tag{28}$$

Next, we note that $\boldsymbol{\theta}_t = \mathbf{H}(\boldsymbol{\theta}_t)^{-1} \Phi_{1:t}^\top \mathbf{y}_{1:t}$, therefore, we can write

$$\begin{aligned}\mathcal{K}_t(\boldsymbol{\theta}; \mathbf{U}_t, \mathbf{W}_t) &= \frac{1}{2}(\boldsymbol{\theta} - \boldsymbol{\theta}_t)^\top \mathbf{H}(\boldsymbol{\theta}_t) (\boldsymbol{\theta} - \boldsymbol{\theta}_t) \\ &= \frac{1}{2}\boldsymbol{\theta}^\top \mathbf{H}(\boldsymbol{\theta}_t) \boldsymbol{\theta} - \boldsymbol{\theta}^\top \mathbf{H}(\boldsymbol{\theta}_t) \boldsymbol{\theta}_t + \text{cnst.} \\ &= \frac{1}{2}\delta_t\|\boldsymbol{\theta}\|^2 + \frac{1}{2}\boldsymbol{\theta}^\top \Phi_{1:t} \Phi_{1:t}^\top \boldsymbol{\theta} - \boldsymbol{\theta}^\top \Phi_{1:t}^\top \mathbf{y}_{1:t} + \text{cnst.} \\ &= \frac{1}{2}\delta_t\|\boldsymbol{\theta}\|^2 + \sum_{j=1}^t \sum_{i \in \mathcal{D}_j} \frac{1}{2}(y_i - \phi_k^\top \boldsymbol{\theta})^2 + \text{cnst.} \\ &= \sum_{j=0}^t \bar{\ell}_j(\boldsymbol{\theta}; \mathcal{D}_j)\end{aligned}\tag{29}$$

This completes the proof.

A.2 Details of PPCA and EM algorithm

The marginal likelihood in Eq. 18 is obtained by noting that, if we marginalize out \mathbf{z}_i and \mathbf{e}_i , then $\mathbf{t}_i \sim \mathcal{N}(0, \mathbf{C})$. Since all \mathbf{t}_i are identically distributed, the likelihood is simply a sum:

$$\begin{aligned}\log p(\mathbf{T}|\mathbf{U}_{t+1}, \mathbf{W}_{t+1}) &= \sum_{i=1}^N \log \mathcal{N}(\mathbf{t}_i|0, \mathbf{C}) = - \sum_{i=1}^N \left[\frac{1}{2} \log |\mathbf{C}| + \frac{1}{2} \mathbf{t}_i^\top \mathbf{C}^{-1} \mathbf{t}_i \right] + \text{cnst.} \\ &= -\frac{1}{2} \left[N \log |\mathbf{C}| + \text{Tr} \left(\mathbf{C}^{-1} \mathbf{T} \mathbf{T}^\top \right) \right] + \text{cnst.}\end{aligned}\tag{30}$$

The stationarity condition can be derived by taking derivative with respect to $\tilde{\mathbf{U}} = \mathbf{U}_{t+1} \mathbf{W}_{t+1}^{1/2}$:

$$(\mathbf{C}^{-1} \mathbf{T} \mathbf{T}^\top \mathbf{C}^{-1} \tilde{\mathbf{U}} - N \mathbf{C}^{-1} \tilde{\mathbf{U}}) = 0 \implies \mathbf{T} \mathbf{T}^\top \mathbf{C}^{-1} \tilde{\mathbf{U}} = N \tilde{\mathbf{U}}, \implies \mathbf{C} = \mathbf{T} \mathbf{T}^\top / N, \tag{31}$$

where the last expression holds when $\tilde{\mathbf{U}}$ has full rank.

The EM algorithm is obtained by noting that the posterior of \mathbf{z}_i is also a Gaussian

$$\mathbf{z}_i | \mathbf{t}_i \sim \mathcal{N}(\mathbf{M}_{t+1}^{-1} \tilde{\mathbf{U}}_{t+1}^\top \mathbf{t}_i, \epsilon \mathbf{M}_{t+1}^{-1}), \tag{32}$$

where $\mathbf{M}_{t+1} = \tilde{\mathbf{U}}_{t+1}^\top \tilde{\mathbf{U}}_{t+1} + \epsilon \mathbf{I}$; see Tipping and Bishop [1999b, Eq. 6]. Using the mean and covariance of this Gaussian in the following M-step, we get

$$\begin{aligned}\tilde{\mathbf{U}}_{t+1} &\leftarrow \left(\sum_{i=1}^N \mathbf{t}_i \mathbb{E}[\mathbf{z}_i]^\top \right) \left(\sum_{i=1}^N \mathbb{E}[\mathbf{z}_i \mathbf{z}_i^\top] \right)^{-1} \\ &= \left(\sum_{i=1}^N \mathbf{t}_i \mathbf{t}_i^\top \tilde{\mathbf{U}}_{t+1} \mathbf{M}_{t+1}^{-1} \right) \left(\sum_{i=1}^N \left[\epsilon \mathbf{M}_{t+1}^{-1} + \mathbf{M}_{t+1}^{-1} \tilde{\mathbf{U}}_{t+1}^\top \mathbf{t}_i \mathbf{t}_i^\top \tilde{\mathbf{U}}_{t+1} \mathbf{M}_{t+1}^{-1} \right] \right)^{-1} \\ &= \tilde{\mathbf{S}} \tilde{\mathbf{U}}_{t+1} \mathbf{M}_{t+1}^{-1} \left(\epsilon \mathbf{M}_{t+1}^{-1} + \mathbf{M}_{t+1}^{-1} \tilde{\mathbf{U}}_{t+1}^\top \tilde{\mathbf{S}} \tilde{\mathbf{U}}_{t+1} \mathbf{M}_{t+1}^{-1} \right)^{-1} \\ &= \tilde{\mathbf{S}} \tilde{\mathbf{U}}_{t+1} \left(\epsilon \mathbf{I} + \mathbf{M}_{t+1}^{-1} \tilde{\mathbf{U}}_{t+1}^\top \tilde{\mathbf{S}} \tilde{\mathbf{U}}_{t+1} \right)^{-1}.\end{aligned}\tag{33}$$

This is the update shown in Eq. 19.

A.3 Details of Hessian Matching for Binary Logistic Regression

We derive the Hessian Matching equation given in Eq. 21. For binary logistic regression, the Hessian with respect to θ is of size $P \times P$. We start by writing the expression for the Hessian of $\ell_{t+1}(\theta; \mathcal{D}_{t+1})$,

$$\frac{\partial^2 \bar{\ell}_{t+1}(\theta_{t+1}; \mathcal{D}_{t+1})}{\partial \theta \partial \theta^\top} = \sum_{j \in \mathcal{D}_{t+1}} \hat{y}'(\phi_j^\top \theta_{t+1}) \phi_j \phi_j^\top \quad (34)$$

where $\hat{y}'(f) = \sigma(f)[1 - \sigma(f)]$. The sum can be written conveniently in a $P \times P$ matrix form by defining a diagonal matrix \mathbf{B}_{t+1} , as shown below:

$$\Phi_{t+1} \mathbf{B}_{t+1} \Phi_{t+1}^\top = \Phi_{t+1} \begin{pmatrix} \hat{y}'(\phi_1^\top \theta_{t+1}) & 0 & \dots & 0 \\ 0 & \hat{y}'(\phi_2^\top \theta_{t+1}) & \dots & 0 \\ \vdots & \vdots & \ddots & \vdots \\ 0 & 0 & \dots & \hat{y}'(\phi_N^\top \theta_{t+1}) \end{pmatrix} \Phi_{t+1}^\top,$$

where we denote the number of examples in \mathcal{D}_{t+1} by N . Similarly, the Hessian of the K-prior is

$$\begin{aligned} \frac{\partial^2 \mathcal{K}_t(\theta_{t+1}; \mathbf{U}_t, \mathbf{w}_t)}{\partial \theta \partial \theta^\top} &= \frac{1}{2} \delta_t \mathbf{I}_P + \sum_{k=1}^{K_t} w_{k|t} \hat{y}'(\mathbf{u}_{k|t}^\top \theta_{t+1}) \mathbf{u}_{k|t} \mathbf{u}_{k|t}^\top \\ &= \frac{1}{2} \delta_t \mathbf{I}_P + \mathbf{U}_t \begin{pmatrix} w_{1|t} \hat{y}'(\mathbf{u}_{1|t}^\top \theta_{t+1}) & 0 & \dots & 0 \\ 0 & w_{2|t} \hat{y}'(\mathbf{u}_{2|t}^\top \theta_{t+1}) & \dots & 0 \\ \vdots & \vdots & \ddots & \vdots \\ 0 & 0 & \dots & w_{K_t|t} \hat{y}'(\mathbf{u}_{K_t|t}^\top \theta_{t+1}) \end{pmatrix} \mathbf{U}_t^\top. \end{aligned} \quad (35)$$

We will denote the diagonal matrix by $\tilde{\mathbf{W}}_t$. The Hessian for the K-prior at task $t + 1$ is obtained in a similar fashion. Using these Hessians, we get the condition given in Eq. 21.

A.4 Details of Hessian Matching for Multi-Class Logistic Regression

For multi-class logistic regression, the Hessian with respect to vectorized Θ is of size $PC \times PC$. To simplify this, we will write the expression in terms of a block corresponding to the second derivative with respect to $\theta^{(c)}$ and $\theta^{(c')}$ which is of size $P \times P$. In total, there are C^2 such blocks for all pairs of (c, c') , using which the full Hessian can be obtained.

As before, we start by writing the expression for the Hessian of $\ell_{t+1}(\theta; \mathcal{D}_{t+1})$,

$$\frac{\partial^2 \bar{\ell}_{t+1}(\Theta; \mathcal{D}_{t+1})}{\partial \theta^{(c)} \partial \theta^{(c')^\top} } = \sum_{j \in \mathcal{D}_{t+1}} [\hat{y}'(\Theta \phi_j)]^{(c, c')} \phi_j \phi_j^\top \quad (36)$$

where $[\hat{y}'(\Theta \phi_j)]^{(c, c')}$ denotes the entry (c, c') of the $P \times P$ matrix $\hat{y}'(\Theta \mathbf{u}_{k|t})$. This can be written conveniently in a $P \times P$ matrix form by defining a diagonal matrix $\mathbf{B}_{t+1}^{(c, c')}$ at Θ_{t+1} , as shown below:

$$\Phi_{t+1} \mathbf{B}_{t+1}^{(c, c')} \Phi_{t+1}^\top = \Phi_{t+1} \begin{pmatrix} [\hat{y}'(\Theta_{t+1} \phi_1)]^{(c, c')} & 0 & \dots & 0 \\ 0 & [\hat{y}'(\Theta_{t+1} \phi_2)]^{(c, c')} & \dots & 0 \\ \vdots & \vdots & \ddots & \vdots \\ 0 & 0 & \dots & [\hat{y}'(\Theta_{t+1} \phi_N)]^{(c, c')} \end{pmatrix} \Phi_{t+1}^\top.$$

Next, we write the K-prior at task t ,

$$\mathcal{K}_t(\Theta; \mathbf{U}_t, \mathbf{w}_t) = \sum_{c=1}^C \delta_t \|\theta^{(c)} - \theta_t^{(c)}\|^2 + \sum_{k=1}^{K_t} w_{k|t} \mathcal{L}(\hat{y}(\Theta_t \mathbf{u}_{k|t}), \hat{y}(\Theta \mathbf{u}_{k|t})). \quad (37)$$

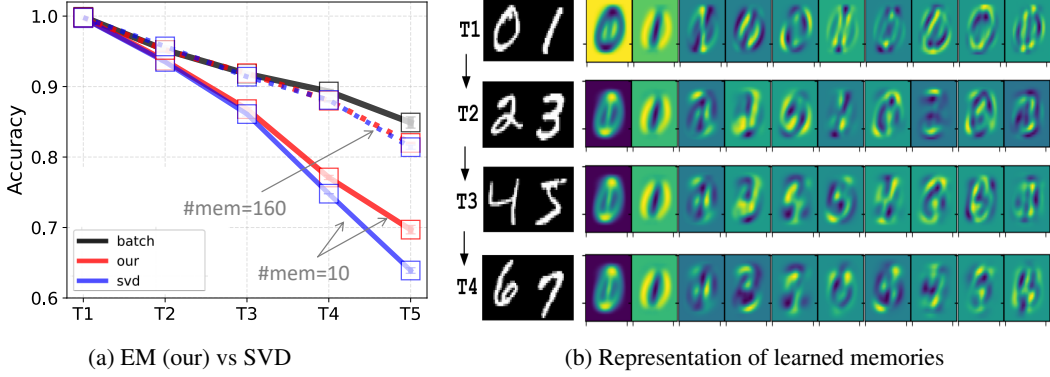


Figure 7: In (a) we compare our method with the SVD approach and batch training (oracle) on a multi-label regression task under two memory scenarios: small (10) and large (160). Our method achieves nearly the same accuracy as the SVD approach in both memory scenarios. However, for Tasks 4 and 5, our method with a small memory size outperforms the SVD approach, suggesting superior numerical robustness to gradient reconstruction errors caused by limited memory. In (b) we visualize the memories as more tasks are added. Each row shows the eigenimages sorted in decreasing eigenvalues from left to right. The first 2 images are consistent, and the left images with smaller eigenvalues (3rd image onward) show the merged features of digits as a new task is learned.

The Hessian is given by following (we denote the indicator by $\mathbb{I}(c = c')$ which is 1 when $c = c'$),

$$\begin{aligned} \frac{\partial^2 \mathcal{K}_t(\Theta; \mathbf{U}_t, \mathbf{w}_t)}{\partial \theta^{(c)} \partial \theta^{(c')\top}} &= \frac{1}{2} \mathbb{I}(c = c') \delta_t \mathbf{I}_P + \sum_{k=1}^{K_t} w_{k|t} [\hat{y}'(\Theta \mathbf{u}_{k|t})]^{(c,c')} \mathbf{u}_{k|t} \mathbf{u}_{k|t}^\top = \frac{1}{2} \mathbb{I}(c = c') \delta_t \mathbf{I}_P \\ &+ \mathbf{U}_t \begin{pmatrix} w_{1|t} [\hat{y}'(\Theta \mathbf{u}_{1|t})]^{(c,c')} & 0 & \dots & 0 \\ 0 & w_{2|t} [\hat{y}'(\Theta \mathbf{u}_{2|t})]^{(c,c')} & \dots & 0 \\ \vdots & \vdots & \ddots & \vdots \\ 0 & 0 & \dots & w_{K_t|t} [\hat{y}'(\Theta \mathbf{u}_{K_t|t})]^{(c,c')} \end{pmatrix} \mathbf{U}_t^\top. \end{aligned} \quad (38)$$

We will denote the diagonal matrix at θ_{t+1} by $\tilde{\mathbf{W}}_t^{(c,c')}$. The K-prior at task $t + 1$ is defined in a similar fashion. Now, applying Hessian matching, we get the following condition for all (c, c') pair:

$$\mathbf{U}_{t+1} \tilde{\mathbf{W}}_{t+1}^{(c,c')} \mathbf{U}_{t+1}^\top + \mathbb{I}(c = c') \epsilon_{t+1} \mathbf{I} = \Phi_{t+1} \mathbf{B}_{t+1}^{(c,c')} \Phi_{t+1}^\top + \mathbf{U}_t \tilde{\mathbf{W}}_t^{(c,c')} \mathbf{U}_t^\top, \quad (39)$$

There are C^2 such conditions, each involving a $P \times P$ matrix. Since one such condition is sufficient, We choose to match the sum over C conditions for the pair (c, c) , that is, when $c = c'$. The advantage of this choice is that the form of Hessian matching is similar to the binary case. The only modification needed is to compute the diagonal matrices by summing of the matrix $\hat{y}'(\mathbf{f})$, which gives rise to the matrices shown in Eq. 27.

B Experiment Details

Our code is available at https://github.com/team-approx-bayes/compact_memory_code. For all experiments, we use NVIDIA RTX 6000 Ada for experiments on Permuted-MNIST and Split-TinyImageNet. For other experiments, we use NVIDIA RTX-3090.

B.1 Multi-Output Regression on Split-MNIST

Experiment setting. We consider the following hyperparameters:

- For feature map $\phi(\mathbf{x})$, we use the identity map where the raw pixel values of the image serve directly as features.

Table 1: The result on the Split-MNIST task: the performance of batch training is 0.849 ± 0.008 .

#Memory	10	20	40	160	320
Our	0.697 ± 0.004	0.744 ± 0.001	0.798 ± 0.000	0.820 ± 0.000	0.815 ± 0.001
SVD	0.639 ± 0.002	0.685 ± 0.003	0.745 ± 0.001	0.815 ± 0.002	0.828 ± 0.002

- For hyperparameters of learning model parameter θ_t , we use Adam optimizer with learning $\text{lr} = 10^{-3}$. We use 100 epochs for each task. For the weight-space regularization hyperparameter δ , we use $\delta = 0.01$.
- For hyperparameters of learning memory \mathbf{U}_{t+1} , we run 10,000 iterations for each task. For the noise hyperparameter ϵ for the EM algorithm, we use $\epsilon = 10^{-3}$.

Multi-output linear regression We show that our EM algorithm for Hessian matching achieves compact memory. We conduct a continual multi-label regression task on **Split-MNIST** [Zenke et al., 2017], where the MNIST dataset is divided into five subsets, each corresponding to a binary classification task with label pairs (0,1), (2,3), (4,5), (6,7), and (8,9). To formulate the binary classification task as a regression problem, we map each label $k \in \{0, \dots, 9\}$ into a vector $\mathbf{1}_k - \frac{1}{10}\mathbf{1}$ where $\mathbf{1}_k \in \mathbb{R}^{10}$ is a one-hot vector with only the k th component set to one and all others set to zero, and $\mathbf{1} \in \mathbb{R}^{10}$ is a vector of ones. For the feature map, we use $\phi(x) = x \in \mathbb{R}^{784}$, that is, the vectorized pixel intensities of an image. For the memory, we use constant memory size per task and accumulate its size as the model trains on new task. After training the model, we measure the classification accuracy using the entire test dataset for evaluation.

Table 1 shows the averaged accuracy of our method with the SVD approach over three seeds across memory size $\{10, 20, 40, 160, 320\}$ to investigate the memory efficiency of our method. The SVD approach obtains memory \mathbf{U}_{t+1} by applying SVD to the right side of Eq.(15). Additionally, we report the result of the batch training, meaning that all tasks are trained without sequentially updating the memory and thus is regarded as the oracle performance. This result shows that our EM method is more effective than the SVD approach when using a smaller memory size (10, 20, and 40).

Fig. 7a compares our method with the SVD approach using memory sizes 10, 160, evaluated after each new task, to investigate its effectiveness with smaller memory. The x-axis denotes the task index, and the y-axis represents the average accuracy over Tasks 1 to t for $t = 1, \dots, 5$; for example, the result at T-3 indicates the average accuracy over Tasks 1–3 after training on Task 3. The results show that our method achieves nearly the same accuracy as the SVD approach up to Task 3 and outperforms it on Tasks 4 and 5. This demonstrates the robustness of our method in training later tasks, where gradient reconstruction errors are more likely to accumulate, making it harder to retain the performance on previously learned tasks. This claim is further supported by the additional results in Table 2, which show that the performance of SVD on past Tasks 1 and 2, evaluated after learning the final task, decreases substantially when a smaller memory size is used.

Additional results. Table 2 compares the performances of our method and the SVD approach, which is regarded as the oracle method. For memory size K_{t+1} , the SVD approach obtains the optimal memory

$$\mathbf{U}_{t+1} = \mathbf{U}_{1:K_{t+1}} \text{diag}(\mathbf{d}_{1:K_{t+1}}^{1/2})$$

sequentially where the columns of eigenvectors $\mathbf{U} \in \mathbb{R}^{H \times R}$ with its rank R and the corresponding eigenvalues $\mathbf{d} \in \mathbb{R}_+^R$ are given by $\text{eigh}(\Phi_{t+1} \Phi_{t+1}^\top + \mathbf{U}_t \mathbf{U}_t^\top) = \mathbf{U} \text{diag}(\mathbf{d}) \mathbf{U}^\top$ for the feature matrix $\Phi_{t+1} \in \mathbb{R}^{H \times N_{t+1}}$ and the previous memory $\mathbf{U}_t \in \mathbb{R}^{H \times K_t}$. The ΔMem denotes the memory size allocated per task; for example, if $\Delta \text{Mem} = 10$ is used, the memory increases by 10 for each task.

This result demonstrates that our method is effective in mitigating catastrophic forgetting, especially when using a small amount of memory, because the performance on previous tasks, achieved by our method, tends to be superior to that of the SVD approach.

B.2 Binary Logistic Regression on the Four-Moon Data Set

Experiment setting. We split all data points of Four-moon datasets into 4 tasks of [500, 500, 500, 500] where the task proceeds as shown in Fig. 8.

Table 2: Multi-output regression on Split-MNIST over 3 runs. The performance of batch training is obtained as 0.839, comparable to the **Avg** of each method.

ΔMem	Method	Task 1	Task 2	Task 3	Task 4	Task 5	Avg
10	Ours	0.920 \pm 0.001	0.474 \pm 0.012	0.616 \pm 0.003	0.602 \pm 0.001	0.874 \pm 0.001	0.697 \pm 0.004
	SVD	0.776 \pm 0.011	0.337 \pm 0.005	0.592 \pm 0.006	0.587 \pm 0.004	0.905 \pm 0.002	0.639 \pm 0.002
20	Ours	0.941 \pm 0.000	0.566 \pm 0.001	0.695 \pm 0.002	0.680 \pm 0.003	0.837 \pm 0.000	0.744 \pm 0.001
	SVD	0.831 \pm 0.010	0.417 \pm 0.006	0.652 \pm 0.004	0.641 \pm 0.002	0.884 \pm 0.004	0.685 \pm 0.003
40	Ours	0.959 \pm 0.000	0.689 \pm 0.001	0.740 \pm 0.001	0.786 \pm 0.001	0.816 \pm 0.001	0.798 \pm 0.000
	SVD	0.877 \pm 0.006	0.535 \pm 0.003	0.688 \pm 0.004	0.735 \pm 0.004	0.889 \pm 0.001	0.745 \pm 0.001
160	Ours	0.966 \pm 0.000	0.764 \pm 0.002	0.738 \pm 0.001	0.848 \pm 0.001	0.785 \pm 0.000	0.820 \pm 0.000
	SVD	0.895 \pm 0.006	0.687 \pm 0.006	0.744 \pm 0.002	0.862 \pm 0.003	0.886 \pm 0.001	0.815 \pm 0.002
320	Ours	0.965 \pm 0.000	0.775 \pm 0.002	0.720 \pm 0.001	0.842 \pm 0.001	0.773 \pm 0.001	0.815 \pm 0.001
	SVD	0.901 \pm 0.006	0.730 \pm 0.005	0.751 \pm 0.004	0.874 \pm 0.003	0.887 \pm 0.002	0.828 \pm 0.002

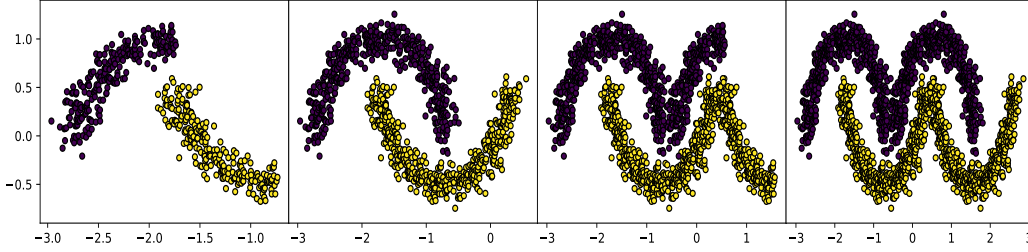


Figure 8: Sequences of four-moon classification task

We consider the following hyperparameters:

- For feature map $\phi(\mathbf{x})$, we use polynomial feature $\text{poly}(5)$ yielding 21 feature dimension. We use the scikit-learn package.
- For hyperparameters of learning model parameter θ_t , we use Adam optimizer with learning $\text{lr} = 0.01$. We set the number of iterations across $\{10000, 20000\}$ to learn the model parameter θ_t for each task; we confirm the convergence of the training loss. For weight-space regularization hyperparameter δ , we set $\delta = 10^{-2}$.
- For hyperparameters of learning memory \mathbf{U}_{t+1} , we set the number of iterations across $\{50, 100, 200\}$ for each task. For the memory size, we consider $\{7, 14, 21\}$ memory for each task and accumulate the memory as the task proceeds. For the noise hyperparameter ϵ , we conduct a grid search over $\epsilon \in \{10^{-3}, 10^{-4}, 10^{-5}\}$ and use 10^{-4} .

Additional results across varying memory size. Fig. 9 shows the results using the 7 and 21 memory per task. The result using 14 memory is reported in Section 4 of the main manuscript. This confirms that our method can match the decision boundary of batch training closely even when using a small amount of memory, as shown in Fig. 9a. As more memory is used, our decision boundary becomes more equal to that of the batch training, as shown in Fig. 9b.

B.3 Binary logistic regression on USPS odd vs even dataset

Experiment setting. We consider the following hyperparameters:

- For feature map $\phi(\mathbf{x})$, we use polynomial feature $\text{poly}(1)$ yielding 256 feature dimension. We use the scikit-learn package.
- For hyperparameters of learning model parameter θ_t , we use Adam optimizer with learning $\text{lr} = 0.1$. We use 5000 iterations to learn the model parameter θ_t for each task. For the weight-space regularization hyperparameter δ , we conduct a grid search over $\delta \in \{0.5, 0.1, 0.05\}$ and use $\delta = 0.5$ for K-prior and our method.
- For hyperparameters of learning memory \mathbf{U}_{t+1} , we use 5000 iterations for each task. For the noise hyperparameter ϵ , we conduct a grid search over $\epsilon \in \{10^{-3}, 10^{-4}, 10^{-5}\}$.

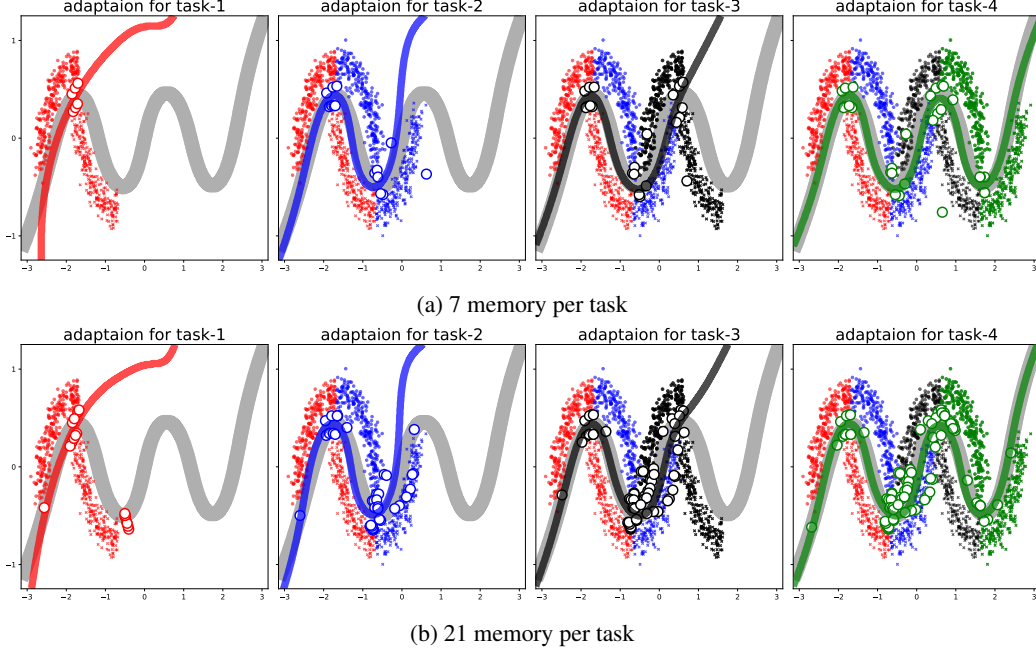


Figure 9: Investigation on varying memory size used for K-prior.

Investigation on varying weight-space regularization hyperparameter for K-prior. Fig. 10 compares K-prior and our method across the varying hyperparameters $\delta \in \{0.5, 0.1, 0.05\}$ that control the importance of weight-space regularization hyperparameter term for K-prior. This result confirms that our method improves the memory efficiency in general and is more effective at $\delta \in \{0.1, 0.05\}$ where the K-prior can match the result of batch training more closely.

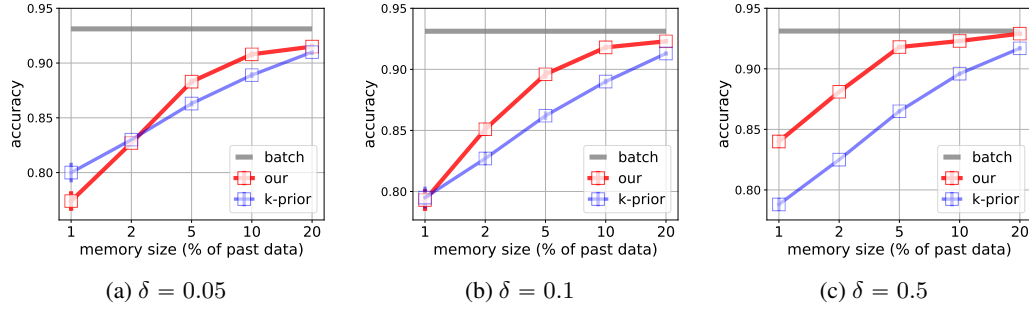


Figure 10: Investigation on varying hyperparameter $\delta \in \{0.05, 0.1, 0.5\}$ for K-prior

Investigation on varying noise hyperparameter EM algorithm for PPCA. Table 3 compares the performances of our method across varying noise hyperparameter ϵ in the EM algorithm for PPCA where we run 5 experiments with different random seeds. This confirms that our method is consistent over the noise hyperparameter ϵ .

B.4 Multi-label Logistic Regression on Split CIFAR-10, CIFAR-100, and TinyImageNet

Experiment setting. We consider the following hyperparameters:

- For feature map $\phi(\mathbf{x})$, we use the feature extractor of ResNet-50 and Vision Transformer (Vit) that are pretrained by CLIP. For Split CIFAR-10, we use Vit-B/32, meaning the base-scale model with 32 patch size. For Split CIFAR-100 and Split Tiny-ImageNet, we use Vit-L/14, meaning the large-scale model size with 14 patch size. The feature extractors of ResNet-50 and Vit yield 2048 features and 768 features, respectively.

Table 3: Investigation on the effect of noise hyperparameter $\epsilon \in \{10^{-3}, 10^{-4}, 10^{-5}\}$.

ΔMem	ϵ	Task 1	Task 2	Task 3	Task 4	Task 5	Avg
1%	$\epsilon = 10^{-3}$	0.769 ± 0.046	0.840 ± 0.012	0.566 ± 0.033	0.982 ± 0.005	0.946 ± 0.002	0.820 ± 0.013
	$\epsilon = 10^{-4}$	0.791 ± 0.029	0.855 ± 0.014	0.623 ± 0.022	0.983 ± 0.003	0.952 ± 0.005	0.840 ± 0.007
	$\epsilon = 10^{-5}$	0.772 ± 0.043	0.872 ± 0.010	0.627 ± 0.032	0.980 ± 0.003	0.954 ± 0.002	0.841 ± 0.008
2%	$\epsilon = 10^{-3}$	0.860 ± 0.010	0.913 ± 0.002	0.689 ± 0.020	0.979 ± 0.003	0.934 ± 0.003	0.875 ± 0.003
	$\epsilon = 10^{-4}$	0.885 ± 0.012	0.885 ± 0.018	0.724 ± 0.008	0.981 ± 0.003	0.933 ± 0.005	0.881 ± 0.004
	$\epsilon = 10^{-5}$	0.891 ± 0.006	0.893 ± 0.012	0.715 ± 0.010	0.982 ± 0.003	0.937 ± 0.002	0.883 ± 0.003
5%	$\epsilon = 10^{-3}$	0.932 ± 0.002	0.931 ± 0.003	0.810 ± 0.011	0.980 ± 0.003	0.920 ± 0.003	0.915 ± 0.002
	$\epsilon = 10^{-4}$	0.950 ± 0.002	0.921 ± 0.003	0.819 ± 0.012	0.983 ± 0.004	0.915 ± 0.005	0.918 ± 0.002
	$\epsilon = 10^{-5}$	0.948 ± 0.002	0.921 ± 0.007	0.798 ± 0.009	0.984 ± 0.002	0.915 ± 0.004	0.913 ± 0.002
10%	$\epsilon = 10^{-3}$	0.933 ± 0.002	0.944 ± 0.005	0.876 ± 0.008	0.972 ± 0.004	0.878 ± 0.003	0.921 ± 0.002
	$\epsilon = 10^{-4}$	0.962 ± 0.002	0.937 ± 0.003	0.855 ± 0.009	0.976 ± 0.003	0.884 ± 0.003	0.923 ± 0.002
	$\epsilon = 10^{-5}$	0.969 ± 0.003	0.934 ± 0.002	0.855 ± 0.009	0.977 ± 0.003	0.889 ± 0.003	0.925 ± 0.001
20%	$\epsilon = 10^{-3}$	0.949 ± 0.003	0.946 ± 0.002	0.891 ± 0.005	0.971 ± 0.002	0.859 ± 0.002	0.923 ± 0.001
	$\epsilon = 10^{-4}$	0.979 ± 0.001	0.949 ± 0.002	0.877 ± 0.006	0.965 ± 0.002	0.872 ± 0.003	0.929 ± 0.002
	$\epsilon = 10^{-5}$	0.981 ± 0.001	0.940 ± 0.001	0.868 ± 0.006	0.967 ± 0.002	0.876 ± 0.004	0.927 ± 0.002

- For hyperparameters of learning model parameter θ_t , we use Adam optimizer with learning lr = 0.1. We use 100 iterations for each task with 1024 batch size. For the weight-space regularization hyperparameter δ , we conduct a grid search over $\delta \in \{0.1, 0.01, 0.001\}$.
- For hyperparameters of learning memory \mathbf{U}_{t+1} , we set 10 iterations for each task. For the noise hyperparameter ϵ , we use $\epsilon = 10^{-4}$.

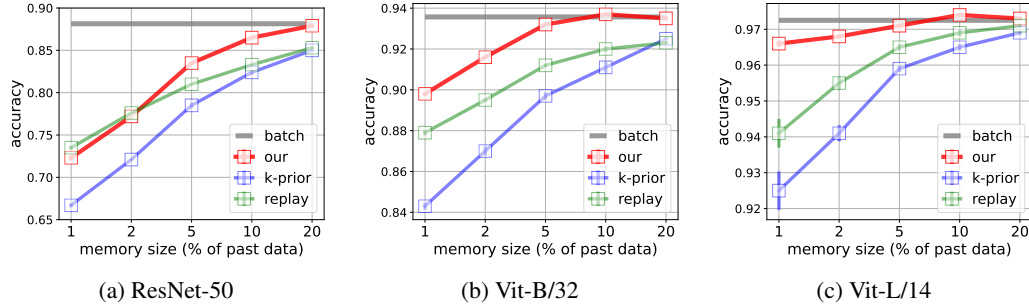


Figure 11: Investigation on varying feature extractor with Split-CIFAR-10.

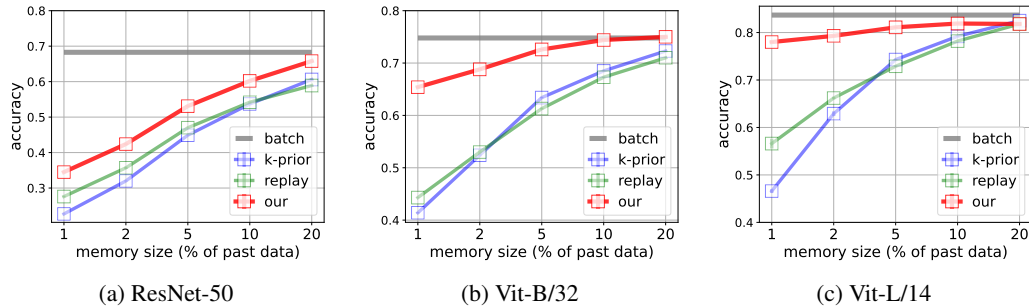


Figure 12: Investigation on varying feature extractor with Split-CIFAR-100.

Investigation on varying feature extractor. Fig. 11 shows the results on Split-CIFAR 10 across varying feature extractors where the feature extractors of ResNet-50, Vit-B/32, and Vit-L/14 are used in Figures 11a to 11c, respectively. Similarly, Figures 12 and 13 show the corresponding results on Split-CIFAR-100 and Split-TinyImageNet, respectively. These results confirm that our method improves memory efficiency consistently regardless of the feature extractor.



Figure 13: Investigation on varying feature extractor with Split-TinyImageNet.

B.5 Additional Results on Permuted MNIST

Experiment setting. Following the benchmark experiment setting in [Carta et al., 2023], we also consider Permuted-MNIST consisting of a sequence of 5 tasks constructed by permuting pixels of 60,000 training samples of MNIST for each task.

We consider the following hyperparameters:

- For feature map $\phi(\mathbf{x})$, we use the feature extractor of ResNet-50 and Vision Transformer (ViT) that are pretrained by CLIP. The feature extractor of ResNet-50 and ViT yield 2048 features and 768 features, respectively
- For hyperparameters of learning model parameter θ_t , we use Adam optimizer with learning $\text{lr} = 0.1$. We use 200 iterations for each task. For the weight-space regularization hyperparameter δ , we conduct a grid search over $\delta \in \{0.01, 0.001\}$.
- For hyperparameters of learning memory \mathbf{U}_{t+1} , we set 10 iterations for each task. For the noise hyperparameter ϵ , we consider $\epsilon = 10^{-4}$.

Additional results. Table 4 shows that our method outperforms other baselines, especially when 1, 2, and 5 percent of data points are used as memory. This result confirms that our method also improves memory efficiency on a domain incremental task.

Table 4: Performance on Permuted-MNIST across varying amount of memory.

Feature	Method	1%	2%	5%	10%
ResNet-50	Replay	0.474 ± 0.002	0.508 ± 0.002	0.554 ± 0.001	$\mathbf{0.592} \pm 0.002$
	K-prior	0.465 ± 0.003	0.493 ± 0.002	0.534 ± 0.002	0.572 ± 0.003
	Our	$\mathbf{0.490} \pm 0.001$	$\mathbf{0.521} \pm 0.001$	$\mathbf{0.561} \pm 0.002$	$\mathbf{0.592} \pm 0.003$
ViT-B/32	Replay	0.490 ± 0.003	0.524 ± 0.002	0.578 ± 0.004	$\mathbf{0.623} \pm 0.003$
	K-prior	0.453 ± 0.001	0.489 ± 0.003	0.549 ± 0.005	0.594 ± 0.004
	Our	$\mathbf{0.522} \pm 0.006$	$\mathbf{0.545} \pm 0.007$	$\mathbf{0.584} \pm 0.003$	0.613 ± 0.004

NeurIPS Paper Checklist

1. Claims

Question: Do the main claims made in the abstract and introduction accurately reflect the paper's contributions and scope?

Answer: [\[Yes\]](#)

Justification: Our work focuses on finding compact memory for continual logistic regression and showing its effectiveness.

Guidelines:

- The answer NA means that the abstract and introduction do not include the claims made in the paper.
- The abstract and/or introduction should clearly state the claims made, including the contributions made in the paper and important assumptions and limitations. A No or NA answer to this question will not be perceived well by the reviewers.
- The claims made should match theoretical and experimental results, and reflect how much the results can be expected to generalize to other settings.
- It is fine to include aspirational goals as motivation as long as it is clear that these goals are not attained by the paper.

2. Limitations

Question: Does the paper discuss the limitations of the work performed by the authors?

Answer: [\[Yes\]](#)

Justification: We mention method of our approach in section of Discussion.

Guidelines:

- The answer NA means that the paper has no limitation while the answer No means that the paper has limitations, but those are not discussed in the paper.
- The authors are encouraged to create a separate "Limitations" section in their paper.
- The paper should point out any strong assumptions and how robust the results are to violations of these assumptions (e.g., independence assumptions, noiseless settings, model well-specification, asymptotic approximations only holding locally). The authors should reflect on how these assumptions might be violated in practice and what the implications would be.
- The authors should reflect on the scope of the claims made, e.g., if the approach was only tested on a few datasets or with a few runs. In general, empirical results often depend on implicit assumptions, which should be articulated.
- The authors should reflect on the factors that influence the performance of the approach. For example, a facial recognition algorithm may perform poorly when image resolution is low or images are taken in low lighting. Or a speech-to-text system might not be used reliably to provide closed captions for online lectures because it fails to handle technical jargon.
- The authors should discuss the computational efficiency of the proposed algorithms and how they scale with dataset size.
- If applicable, the authors should discuss possible limitations of their approach to address problems of privacy and fairness.
- While the authors might fear that complete honesty about limitations might be used by reviewers as grounds for rejection, a worse outcome might be that reviewers discover limitations that aren't acknowledged in the paper. The authors should use their best judgment and recognize that individual actions in favor of transparency play an important role in developing norms that preserve the integrity of the community. Reviewers will be specifically instructed to not penalize honesty concerning limitations.

3. Theory Assumptions and Proofs

Question: For each theoretical result, does the paper provide the full set of assumptions and a complete (and correct) proof?

Answer: [NA]

Justification: Our work does not have a theoretical result and focuses on showing empirical improvement of the proposed algorithm.

Guidelines:

- The answer NA means that the paper does not include theoretical results.
- All the theorems, formulas, and proofs in the paper should be numbered and cross-referenced.
- All assumptions should be clearly stated or referenced in the statement of any theorems.
- The proofs can either appear in the main paper or the supplemental material, but if they appear in the supplemental material, the authors are encouraged to provide a short proof sketch to provide intuition.
- Inversely, any informal proof provided in the core of the paper should be complemented by formal proofs provided in appendix or supplemental material.
- Theorems and Lemmas that the proof relies upon should be properly referenced.

4. Experimental Result Reproducibility

Question: Does the paper fully disclose all the information needed to reproduce the main experimental results of the paper to the extent that it affects the main claims and/or conclusions of the paper (regardless of whether the code and data are provided or not)?

Answer: [Yes]

Justification: We describe experiment configuration in Appendix B.

Guidelines:

- The answer NA means that the paper does not include experiments.
- If the paper includes experiments, a No answer to this question will not be perceived well by the reviewers: Making the paper reproducible is important, regardless of whether the code and data are provided or not.
- If the contribution is a dataset and/or model, the authors should describe the steps taken to make their results reproducible or verifiable.
- Depending on the contribution, reproducibility can be accomplished in various ways. For example, if the contribution is a novel architecture, describing the architecture fully might suffice, or if the contribution is a specific model and empirical evaluation, it may be necessary to either make it possible for others to replicate the model with the same dataset, or provide access to the model. In general, releasing code and data is often one good way to accomplish this, but reproducibility can also be provided via detailed instructions for how to replicate the results, access to a hosted model (e.g., in the case of a large language model), releasing of a model checkpoint, or other means that are appropriate to the research performed.
- While NeurIPS does not require releasing code, the conference does require all submissions to provide some reasonable avenue for reproducibility, which may depend on the nature of the contribution. For example
 - (a) If the contribution is primarily a new algorithm, the paper should make it clear how to reproduce that algorithm.
 - (b) If the contribution is primarily a new model architecture, the paper should describe the architecture clearly and fully.
 - (c) If the contribution is a new model (e.g., a large language model), then there should either be a way to access this model for reproducing the results or a way to reproduce the model (e.g., with an open-source dataset or instructions for how to construct the dataset).
 - (d) We recognize that reproducibility may be tricky in some cases, in which case authors are welcome to describe the particular way they provide for reproducibility. In the case of closed-source models, it may be that access to the model is limited in some way (e.g., to registered users), but it should be possible for other researchers to have some path to reproducing or verifying the results.

5. Open access to data and code

Question: Does the paper provide open access to the data and code, with sufficient instructions to faithfully reproduce the main experimental results, as described in supplemental material?

Answer: [Yes]

Justification: We will attach our implementation and share it using anonymous Github.

Guidelines:

- The answer NA means that paper does not include experiments requiring code.
- Please see the NeurIPS code and data submission guidelines (<https://nips.cc/public/guides/CodeSubmissionPolicy>) for more details.
- While we encourage the release of code and data, we understand that this might not be possible, so “No” is an acceptable answer. Papers cannot be rejected simply for not including code, unless this is central to the contribution (e.g., for a new open-source benchmark).
- The instructions should contain the exact command and environment needed to run to reproduce the results. See the NeurIPS code and data submission guidelines (<https://nips.cc/public/guides/CodeSubmissionPolicy>) for more details.
- The authors should provide instructions on data access and preparation, including how to access the raw data, preprocessed data, intermediate data, and generated data, etc.
- The authors should provide scripts to reproduce all experimental results for the new proposed method and baselines. If only a subset of experiments are reproducible, they should state which ones are omitted from the script and why.
- At submission time, to preserve anonymity, the authors should release anonymized versions (if applicable).
- Providing as much information as possible in supplemental material (appended to the paper) is recommended, but including URLs to data and code is permitted.

6. Experimental Setting/Details

Question: Does the paper specify all the training and test details (e.g., data splits, hyperparameters, how they were chosen, type of optimizer, etc.) necessary to understand the results?

Answer:[Yes]

Justification: We describe experiment configuration in Appendix B.

Guidelines:

- The answer NA means that the paper does not include experiments.
- The experimental setting should be presented in the core of the paper to a level of detail that is necessary to appreciate the results and make sense of them.
- The full details can be provided either with the code, in appendix, or as supplemental material.

7. Experiment Statistical Significance

Question: Does the paper report error bars suitably and correctly defined or other appropriate information about the statistical significance of the experiments? [Yes]

Justification: We obtain statistically significant results after multiple runs with different random seeds for all experiments.

Guidelines:

- The answer NA means that the paper does not include experiments.
- The authors should answer "Yes" if the results are accompanied by error bars, confidence intervals, or statistical significance tests, at least for the experiments that support the main claims of the paper.
- The factors of variability that the error bars are capturing should be clearly stated (for example, train/test split, initialization, random drawing of some parameter, or overall run with given experimental conditions).
- The method for calculating the error bars should be explained (closed form formula, call to a library function, bootstrap, etc.)

- The assumptions made should be given (e.g., Normally distributed errors).
- It should be clear whether the error bar is the standard deviation or the standard error of the mean.
- It is OK to report 1-sigma error bars, but one should state it. The authors should preferably report a 2-sigma error bar than state that they have a 96% CI, if the hypothesis of Normality of errors is not verified.
- For asymmetric distributions, the authors should be careful not to show in tables or figures symmetric error bars that would yield results that are out of range (e.g. negative error rates).
- If error bars are reported in tables or plots, The authors should explain in the text how they were calculated and reference the corresponding figures or tables in the text.

8. Experiments Compute Resources

Question: For each experiment, does the paper provide sufficient information on the computer resources (type of compute workers, memory, time of execution) needed to reproduce the experiments?

Answer: [Yes]

Justification: We describe experiment configuration in Appendix.

Guidelines:

- The answer NA means that the paper does not include experiments.
- The paper should indicate the type of compute workers CPU or GPU, internal cluster, or cloud provider, including relevant memory and storage.
- The paper should provide the amount of compute required for each of the individual experimental runs as well as estimate the total compute.
- The paper should disclose whether the full research project required more compute than the experiments reported in the paper (e.g., preliminary or failed experiments that didn't make it into the paper).

9. Code Of Ethics

Question: Does the research conducted in the paper conform, in every respect, with the NeurIPS Code of Ethics <https://neurips.cc/public/EthicsGuidelines>?

Answer: [Yes]

Justification: We follow the NeurIPS Code of Ethics.

Guidelines:

- The answer NA means that the authors have not reviewed the NeurIPS Code of Ethics.
- If the authors answer No, they should explain the special circumstances that require a deviation from the Code of Ethics.
- The authors should make sure to preserve anonymity (e.g., if there is a special consideration due to laws or regulations in their jurisdiction).

10. Broader Impacts

Question: Does the paper discuss both potential positive societal impacts and negative societal impacts of the work performed?

Answer: [NA]

Justification: Our work is expected to advance continual adaptation procedure effectively, but it seems to have limited relevance to broader societal impacts.

Guidelines:

- The answer NA means that there is no societal impact of the work performed.
- If the authors answer NA or No, they should explain why their work has no societal impact or why the paper does not address societal impact.
- Examples of negative societal impacts include potential malicious or unintended uses (e.g., disinformation, generating fake profiles, surveillance), fairness considerations (e.g., deployment of technologies that could make decisions that unfairly impact specific groups), privacy considerations, and security considerations.

- The conference expects that many papers will be foundational research and not tied to particular applications, let alone deployments. However, if there is a direct path to any negative applications, the authors should point it out. For example, it is legitimate to point out that an improvement in the quality of generative models could be used to generate deepfakes for disinformation. On the other hand, it is not needed to point out that a generic algorithm for optimizing neural networks could enable people to train models that generate Deepfakes faster.
- The authors should consider possible harms that could arise when the technology is being used as intended and functioning correctly, harms that could arise when the technology is being used as intended but gives incorrect results, and harms following from (intentional or unintentional) misuse of the technology.
- If there are negative societal impacts, the authors could also discuss possible mitigation strategies (e.g., gated release of models, providing defenses in addition to attacks, mechanisms for monitoring misuse, mechanisms to monitor how a system learns from feedback over time, improving the efficiency and accessibility of ML).

11. Safeguards

Question: Does the paper describe safeguards that have been put in place for responsible release of data or models that have a high risk for misuse (e.g., pretrained language models, image generators, or scraped datasets)?

Answer: [NA]

Justification: this paper poses no such risks.

Guidelines:

- The answer NA means that the paper poses no such risks.
- Released models that have a high risk for misuse or dual-use should be released with necessary safeguards to allow for controlled use of the model, for example by requiring that users adhere to usage guidelines or restrictions to access the model or implementing safety filters.
- Datasets that have been scraped from the Internet could pose safety risks. The authors should describe how they avoided releasing unsafe images.
- We recognize that providing effective safeguards is challenging, and many papers do not require this, but we encourage authors to take this into account and make a best faith effort.

12. Licenses for existing assets

Question: Are the creators or original owners of assets (e.g., code, data, models), used in the paper, properly credited and are the license and terms of use explicitly mentioned and properly respected?

Answer: [NA]

Justification: this paper does not use existing assets.

Guidelines:

- The answer NA means that the paper does not use existing assets.
- The authors should cite the original paper that produced the code package or dataset.
- The authors should state which version of the asset is used and, if possible, include a URL.
- The name of the license (e.g., CC-BY 4.0) should be included for each asset.
- For scraped data from a particular source (e.g., website), the copyright and terms of service of that source should be provided.
- If assets are released, the license, copyright information, and terms of use in the package should be provided. For popular datasets, paperswithcode.com/datasets has curated licenses for some datasets. Their licensing guide can help determine the license of a dataset.
- For existing datasets that are re-packaged, both the original license and the license of the derived asset (if it has changed) should be provided.

- If this information is not available online, the authors are encouraged to reach out to the asset’s creators.

13. **New Assets**

Question: Are new assets introduced in the paper well documented and is the documentation provided alongside the assets?

Answer: [NA]

Justification: this paper does not release new assets.

Guidelines:

- The answer NA means that the paper does not release new assets.
- Researchers should communicate the details of the dataset/code/model as part of their submissions via structured templates. This includes details about training, license, limitations, etc.
- The paper should discuss whether and how consent was obtained from people whose asset is used.
- At submission time, remember to anonymize your assets (if applicable). You can either create an anonymized URL or include an anonymized zip file.

14. **Crowdsourcing and Research with Human Subjects**

Question: For crowdsourcing experiments and research with human subjects, does the paper include the full text of instructions given to participants and screenshots, if applicable, as well as details about compensation (if any)?

Answer: [NA]

Justification: this paper does not involve crowdsourcing nor research with human subjects.

Guidelines:

- The answer NA means that the paper does not involve crowdsourcing nor research with human subjects.
- Including this information in the supplemental material is fine, but if the main contribution of the paper involves human subjects, then as much detail as possible should be included in the main paper.
- According to the NeurIPS Code of Ethics, workers involved in data collection, curation, or other labor should be paid at least the minimum wage in the country of the data collector.

15. **Institutional Review Board (IRB) Approvals or Equivalent for Research with Human Subjects**

Question: Does the paper describe potential risks incurred by study participants, whether such risks were disclosed to the subjects, and whether Institutional Review Board (IRB) approvals (or an equivalent approval/review based on the requirements of your country or institution) were obtained?

Answer: [NA]

Justification: this paper does not involve crowdsourcing nor research with human subjects

Guidelines:

- The answer NA means that the paper does not involve crowdsourcing nor research with human subjects.
- Depending on the country in which research is conducted, IRB approval (or equivalent) may be required for any human subjects research. If you obtained IRB approval, you should clearly state this in the paper.
- We recognize that the procedures for this may vary significantly between institutions and locations, and we expect authors to adhere to the NeurIPS Code of Ethics and the guidelines for their institution.
- For initial submissions, do not include any information that would break anonymity (if applicable), such as the institution conducting the review.

16. **Declaration of LLM usage**

Question: Does the paper describe the usage of LLMs if it is an important, original, or non-standard component of the core methods in this research? Note that if the LLM is used only for writing, editing, or formatting purposes and does not impact the core methodology, scientific rigorousness, or originality of the research, declaration is not required.

Answer: [NA]

Justification: The LLM is used only for formatting purposes, including figure and tables.

Guidelines:

- The answer NA means that the core method development in this research does not involve LLMs as any important, original, or non-standard components.
- Please refer to our LLM policy (<https://neurips.cc/Conferences/2025/LLM>) for what should or should not be described.